University of Texas at Tyler
Scholar Works at UT Tyler

Electrical Engineering Theses | Electrical Engineering

Fall 1-15-2014

PMU-Based Adaptive Central Protection Unit (CPU) for Power Systems with High DG Penetration

Pooria Mohammadi

Follow this and additional works at: https://scholarworks.uttyler.edu/ee_grad

Part of the Electrical and Computer Engineering Commons

Recommended Citation

Mohammadi, Pooria, "PMU-Based Adaptive Central Protection Unit (CPU) for Power Systems with High DG Penetration" (2014). *Electrical Engineering Theses.* Paper 13.
http://hdl.handle.net/10950/191

This Thesis is brought to you for free and open access by the Electrical Engineering at Scholar Works at UT Tyler. It has been accepted for inclusion in Electrical Engineering Theses by an authorized administrator of Scholar Works at UT Tyler. For more information, please contact tgullings@uttyler.edu.

PMU-BASED ADAPTIVE CENTRAL PROTECTION UNIT (CPU) FOR POWER SYSTEMS WITH HIGH DG PENETRATION

by

POORIA MOHAMMADI

A thesis submitted in partial fulfillment
of the requirement for the degree of
Master of Science in Electrical Engineering
Department of Electrical Engineering

Hassan El-Kishky, Ph.D., P.E., Committee Chair

College of Engineering and Computer Science

The University of Texas at Tyler
November 2013

The University of Texas at Tyler
Tyler, Texas

This is to certify that the Master's Thesis of

POORIA MOHAMMADI

Has been approved for the thesis requirement on
November 11, 2013
For the Master of Science Degree in Electrical Engineering

Approvals:

Thesis Chair: Hassan El-Kishky, Ph.D., P.E.

Member: Ron J. Pieper, Ph.D., P.E.

Member: Hector Ochoa, Ph.D.

Interim Chair, Department of Electrical Engineering:
Hassan El-Kishky, Ph.D., P.E.

Dr. James K. Nelson, Jr., Ph.D., P.E.,
Dean, College of Engineering and Computer Science,

© Copyright by Pooria Mohammadi 2013

All rights reserved

Acknowledgments

I would like to express my sincere gratitude and appreciation to my advisor Dr. Hassan El-Kishky for his professional guidance, constant encouragement, and support. His intellectual and financial support was indispensable for the completion of this thesis. I would also like to thank my committee members, Dr. Ron Pieper and Dr. Hector Ochoa for their valuable insights and continuous support. There are not enough words to describe the amount of help and support that I received from Dr. Alecia Wolf, Ms. Jennifer Knupp, as well as Ms. Kenza El-Amrani. At last, I want to express my sincere appreciation to my wonderful family back home in Iran. Without a doubt, this accomplishment would have never been possible without their continuous support, unconditional love, and prayers. I'd also like to thank Zack Parrish and his wonderful family for their support and encouragement.

Table of Contents

List of Tables ..... **iv**

List of Figures ..... **iii**

Chapter One: Introduction **1**

1.1 Motivation 1

1.2 Thesis Objective 2

1.3 Thesis Structure 3

Chapter Two: Power Systems and Distributed Generation (DG) **4**

2.1 Overview 4

2.2 Power System Structures 4

2.2.1Loop Networks 4

2.2.2 Radial Networks 5

2.3 Power System Protection 6

2.3.1 Over Current Relay R50/51 and R67 7

2.4 Distributed Generation (DG) 10

2.4.1 Wind Turbine 12

2.4.2 Fuel Cell (FC) 13

2.4.3 Photo Voltaic (PV) 14

2.4.4 Synchronous Generator 15

2.5 DGs Interconnections 16

Chapter Three: DGs Integration Impacts **19**

3.1 Overview 19

3.2 Impacts on Power System 20

3.2.1 Structure Alteration 20

3.2.2 Voltage Profile 21

3.2.3 Fault Current Level 25

3.2.4 Fault Current Contribution 28

3.3 Impacts on Protection System 29

3.3.1 IEEE 34-Bus and Protection System 29

3.3.2 Feeders Nominal Current 37

3.3.3 OCR Miscoordination 38

3.3.4 OCR Blinding 40

Chapter Four: Phasor Measurement Unit (PMU) and K-means Clustering **42**

4.1 Overview 42

4.2 PMU Algorithms 43

4.3 Mathematical Principles of DFT and SDFT 44
4.4 DFT and SDFT Comparison.....48
4.5 K-means Clustering 53
4.6 K-means Clustering Principals 54
4.6 Proposed Initialization Algorithm 56
4.7 PMU Data Clustering 61
4.8 Conclusion 64
Chapter Five: CPU for Smart Grids with Decisive Private DGs.....66
5.1 Overview 66
5.2 CPU Description.....67
5.2.1 Off Line Data 67
5.2.2 DGs Environmental Condition 68
5.2.3 Authority Load Priority.....68
5.2.4 Online Data 69
5.3 Conclusion 72
5.4 Future Work.....72
References.....73

List of Tables

Table 3.1 Bus P-Q Values for IEEE 13-Bus…….....…..... 21
Table 3.2 Case Studies……..... 22
Table 3.3 Fault Current in Blackout for Various Faults…….….. 26
Table 3.4 Fault Current Level……... 34
Table 3.5 OCR Miscoordination for Fault at Bus 27……..... 39
Table 3.6 OCR Miscoordination for Fault at Bus 18……..….. 39
Table 3.7 Overcurrent Protection Response……..……... 40
Table 3.8 Overcurrent Protection Response……. 41

List of Figures

Figure 2.1 Power System Distribution Networks Loop Topology..... 4
Figure 2.2 Power System Distribution Networks Radial Topology..... 5
Figure 2.3 OCR 51 Details MATLAB Signal…….……... 8
Figure 2.4 DOCR 67 Details MATLAB Signal…….……..... 9
Figure 2.5 DOCR 67 Details MATLAB Signal…….……..... 10
Figure 2.6 DFIG Wind Turbine…….……. 12
Figure 2.7 FC Electrical Equivalent…….…….…. 13
Figure 2.8 FC Characteristic Curve…….……...… 13
Figure 2.9 FC MATLAB Model…… 14
Figure 2.10 PV Electrical Equivalent…….…… 15
Figure 2.11 PV Characteristic Curve…….……. 15
Figure 2.12 PV MATLAB Model…….…… 15
Figure 2.13 a) IIDG Scheme, b) DC Base IIDG Power Grid Interface……..…… 16
Figure 2.14 Synchronous Generator Responses to Various Fault Scenarios…….…… 18
Figure 2.15 PV Responses to Various Fault Scenarios…….…… 18
Figure 2.16 FC Responses to Various Fault Scenarios…….…… 18
Figure 3.1 IEEE 13-Bus Radial Distribution System……..……... 20
Figure 3.2 a Typical Radial Distribution Feeder Voltage Profile……..…….. 23
Figure 3.3 IEEE 13-Bus Voltage Profile…….……..... 24
Figure 3.4 System Voltage Profile with Fault at Bus 11…….……..... 25
Figure 3.5 DGs Integration in Radial Feeder…….……..… 27
Figure 3.6 a) Equivalent Network with Integrated DG b) Equivalent……..…...…… 27
Figure 3.7 UG's Contribution in 3-ph Bolted Fault at Bus 12……..…….. 28
Figure 3.8 UG Contribution in 3-ph Bolted Fault at Bus 11…….…….…. 29
Figure 3.9 IEEE 34-Bus Distribution Network Test Feeder…….……... 31
Figure 3.10 Voltage Profile for: a)Base Case. b)Syn DG. c) DFIG DG…….…… 33
Figure 3.11Utility Grid Contribution in Fault at Bus 32…….……... 34
Figure 3.12 Utility Grid Contribution after DG Integration...…….……... 35
Figure 3.13 Over Current Relays Allocations Inside Protective Zones…….……..... 36
Figure 3.14 OCR Protection System and Its Detailed Zones and Buses…….…... 37
Figure 3.15 OCR Coordination Curves for Zones I to II…….….. 37
Figure 3.16 OCR Miscoordination for Fault at Bus 27…….…..... 38
Figure 3.17 Fault Current for Fault at Bus …….…... 41
Figure 4.1 Central Protection Unit and PMU Importance…….…. 42
Figure 4.2 DFT and SDFT in off-Nominal Frequency (51Hz)…….…… 48

Figure 4.3 DFT Amplitude Oscillation…… 49
Figure 4.4 5Hz Step Change Response: a)DFT b)SDFT…….... 50
Figure 4.5 2 Hz Ramp Change in Frequency a)DFT b)SDFT……..… 51
Figure 4.6 DFT Amplitude with Ramp Change in Frequency……..…..… 52
Figure 4.7 K-means Basic Algorithm……...….... 56
Figure 4.8 PMU 5 Data for a Scenario……..…….. 57
Figure 4.9 PMU 5 VIϕa 3-D Data Presentation……...… 57
Figure 4.10 Discrete Function D(i) Representing the System Step Length……. 58
Figure 4.11 Proposed Initial Centroids Calculation Algorithm Flowchart…….…. 59
Figure 4.12 PMU 5 Clustered by Basic K-means……..…..... 61
Figure 4.13 PMU 5 Clustered Using Proposed Algorithm…….…… 61
Figure 4.14 PMU 3 Clustered by Basic K-means……...…... 64
Figure 4.15 PMU 5 Clustered Using Proposed Algorithm…….…… 63
Figure 4.16 Clustered Using Proposed Algorithm……...….... 63
Figure 5.1 Central Protection Unit (CPU) Overview…….… 67
Figure 5.2 Central Diagram……..... 68
Figure 5.3 K-means Clustering for a Fault Scenario……...….... 70
Figure 5.4 I Change in DGs Topology……... 70
Figure 5.5 System State Estimation Using Vφf Signals……..... 71
Figure 5.6 a)Kurtosis and b) Skewness Indices…….. 71

Abstract

PMU-BASED ADAPTIVE CENTRAL PROTECTION UNIT (CPU) FOR POWER SYSTEMS WITH HIGH DG PENETRATION

Pooria Mohammadi

Thesis Chair: Hassan El-Kishky, Ph.D., P.E.

The University of Texas at Tyler
November 2013

The rapid expansion and integration of Distributed Generations (DG) into power systems plays an increasingly important role in their planning, operation, and control. The rules used to design and operate current systems are being altered by the DGs incorporation. This may jeopardize the system's reliability and security. Private owners of large DGs should not be restricted to a particular time schedule to connect/disconnect their generation to/from the system. This feature dynamically changes the typical power system with unidirectional power flow from generation to the loads. A smart Central Protection Unit (CPU) is needed to take proper measures in case of DGs arbitrarily disconnection, isolation or any other type of fault. On the other hand, recent major blackouts resulting from pushing the power systems to the edge has revealed the need for a smarter supervisory system for enhanced reliability and stability. Hence, there is a high demand for a robust and smart supervisory system which can diagnose power systems' disturbances in real-time and prevent aggravation and expansion.

This thesis is focused on studying the impacts of DG integration on the power systems. Phasor Measurement Units (PMUs) play an important role on the monitoring of power systems. Multiple major data analysis techniques including K-means, Smart K-means clustering, and DBSCAN clustering of the PMU output data have been implemented. Higher order moments of Kurtosis and Skewness indices were also employed in order to estimate the system state.

Chapter One
Introduction

1.1 Motivation

The power system infrastructure is in an era of transition. Recent advances and the developments in engineering and technology have impacted the way many power professionals perceive a smart and reliable power grid. Carbone Nano-tubes, Nano science, Gallium Nitrate, low-k and high-k materials, super conductors, optical fibers, artificial hearts, and the progress toward space mineral extraction are all examples of the numerous fields in which advances have been made. However, power systems that is one of the most important fields, has not been improving in pace with the rest for one and a half centuries.

The rapid expansion and integration of Distributed Generations (DG) into power systems plays an increasingly important role in their planning, operation, and control. The rules used to design and operate current systems are being altered by the DGs incorporation. This may jeopardize the system's reliability and security [1]. Private owners of large DGs should not be restricted to a particular time schedule to connect/disconnect their generation to/from the system. This feature dynamically changes the typical power system with unidirectional power flow from generation to the loads. A smart Central Protection Unit (CPU) is needed to take proper measures in case of DGs arbitrarily disconnection, isolation or any other type of fault. On the other hand, recent major blackouts resulting from pushing the power systems to the edge has revealed the need for a smarter supervisory system for enhanced reliability and stability. Hence, there is a high demand for a robust and smart supervisory system which can diagnose power systems' disturbances in real-time and prevent aggravation and expansion.

Many issues with the integrated power systems since the 1970s have convinced governments and researchers to move toward Sustainable Energy Resources (SER). These have been known as the best solutions for issues such as high carbon dioxide emissions, ozone layer and environmental concerns, relieving oil-dependent economies, and more importantly, attracting small investors. Utilizing SER generation units enables the industry to manufacture and scatter small generation units all over the power system network, known as Distributed Generation (DG). These units facilitate the use of renewable energies with small capital expenses which makes

it more affordable for private owners. Imagine that every house would have one or two types of DGs like PHEV, Wind Turbine, Photo Voltaic (PV), Fuel Cell (FC), Geothermal unit, diesel or a gas generator, depending on their geographical location [1,2]. This leads us to the point of controlling and supervising the power system rather than generating and transferring the electricity. This is a complicated system containing various DGs with private owners, which may or may not be connected to the network. Therefore it demands an adaptive and intelligent power network for its complexity and dynamic behavior. It is useful to mention that current networks are designed and operated with a specific and fixed structure. Any major change requires a physical action such as sending crew to the site.

Recent wide area power outages mainly resulted from failures in responding to and extinguishing aggravating disturbances in power systems. This clearly shows the demand for drastic reforms and basic changes in power system control and supervision means, methods, and algorithms. On the other hand, integrating various DGs into the power system makes this task more complex by converting the current stationary power systems which have already been pushed to their stability limits into a dynamic power system. The University of Texas at Tyler research group has designed a control and supervisory algorithm for such a dynamic power system named Central Protection Unit (CPU). CPU is a state of the art intelligent power system management and control center scheme which enables us to move toward the unavoidable smart power systems. They take advantage of the latest science, technology, and engineering advances such as super processors, fast, wireless and optic communications, PMU, GPS, SCADA, WAMS, and digital relays [2]. Also, mathematical approaches like Neural Networks, Clustering and Graph Theory have been utilized. The main responsibility of the CPU is to detect the disturbances and system alterations, and subsequently respond with the best possible actions.

1.2 Thesis Objective

This thesis is focused on studying the impacts of DG integration on the power systems. Phasor Measurement Units (PMUs) play an important role on the monitoring of power systems. Multiple major data analysis techniques including K-means, Smart K-means clustering, and DBSCAN clustering of the PMU output data have been implemented. Higher order moments of Kurtosis and Skewness indices were also employed in order to estimate the system state.

The objective of this research work is to establish an adaptive and intelligent Central Protection Unit (CPU) for evolving power systems. The CPU aims to be adaptive enough to employ various DGs into the power systems and prevent scarifying the system security and reliability due to integration impacts. This should be done by remotely manipulating protection system devices such relay characteristics to meet the new situation. Fault and disturbance diagnosis, utilizing PMU technology, and effective islanding are also included in the CPU algorithm and objectives. Various objectives have been considered in order to pave the way toward reaching a robust, smart, and adaptive CPU. The following is a list of the issues addressed in this thesis:

- Evaluating issues about DG integration in power systems
- Narrowly categorizing DG's integration impacts on Distribution Networks.
- PMU's principal mathematic and algorithms accuracy and robustness
- Employing SCADA and WAMS in new proposed CPU.
- Methods for analyzing PMU, SCADA, WAMS and other necessary data acquisition systems
- Neural networks, pattern recognition, and K-means clustering.

1.3 Thesis Structure

Chapter 2 discusses the power system structures, especially in distribution systems, the different DG types, and their various power electronics interconnection. Chapter 3 presents the result yielded by comprehensive simulation for categorizing DGs' integration impacts, especially on distribution networks and how their interconnection may influence these impacts. Chapter 4 introduces and compares various PMUs' algorithms and chooses one as the most suitable and applicable for CPU y providing its mathematical principal along with its simulation results. Additionally, three mathematical methods for analyzing PMUs data have been thoroughly covered. Chapter 5 covers the CPU logic flowcharts and algorithms in employing the discussed methods to intelligently decide about and react to changes in the system or disturbances. The thesis closes with a concise conclusion along with proposed future work.

Chapter Two
Power Systems and Distributed Generation

2.1 Overview

Distributed generation integration is the main point of this thesis. It proposes changes in the principal rules and regulations in which power systems structures currently operate. These changes include changing the power flow direction, current direction, and even the system admittance matrix. Therefore, to build a robust protection system, one should first have a broad knowledge about the network structure and the DGs which are supposed to be integrated. This chapter presents the various power system structures, the different DGs specifications, and their specific characteristics.

2.2 Power System Structures

2.2.1Loop Networks

One of the power systems distribution topology is the loop structure. This structure is a complex topology in terms of design, control, and expansion. This is why protection and compensation equipment for such networks are usually more complicated to design. It takes more time to fulfill the design process which includes the complicated load grow forecast and relative power flow in loop networks comparing to radial. In distribution power systems, the loop structure is referring to a system in which a closed loop path starting from a generation unit can be found.

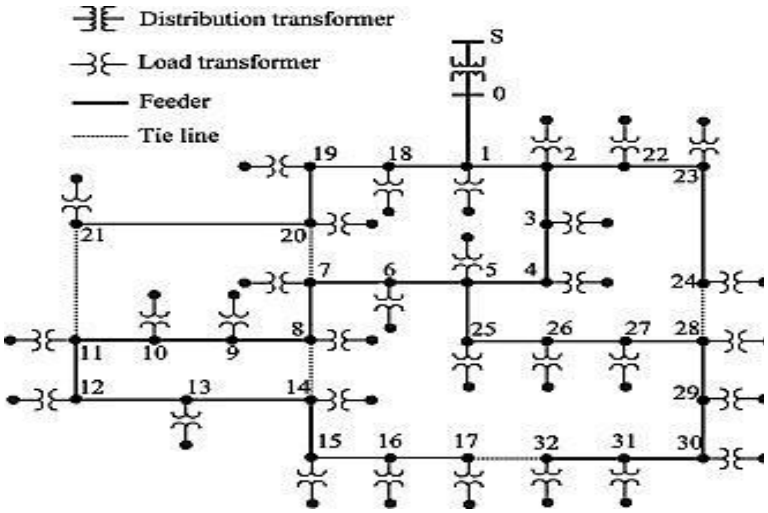

Figure 2.1 Power System Distribution Networks Loop Topology

Figure 2.1 shows a typical loop structure in the power system distribution feeder. One of the loop structure's advantages is the better voltage profile in comparison to that of the radial networks'. The loop structure in Figure 2.1 is feeding from a single point to the utility grid (point S) but a loop structure has the capability to inject power from different loop sides. This reduces the transmission path from the generation to the consumption point, resulting in less power loss and subsequently better and more even voltage profile. Also, designing an overcurrent protection scheme is complicated in these networks and possible just by using directional overcurrent relay (R67). Designing overcurrent protection requires calculating changes in load and generation in order to reach accurate values for current flowing in both directions and at different times. Adding DGs to such a topology increases the complexity, particularly if the DGs are decisive unit with a private owner who arbitrarily determines the time schedule for being coupled with the network.

2.2.2 Radial Networks

One of the famous topologies which power systems fell into is radial networks. Radial networks are well known in power systems because of their long time and wide area applications. They have been used in power systems since the very beginning because of their ease of design and simplicity in their compensations. Radial feeders are networks in which there is a single path from the generation point to the loads. Figure 2.2 shows a typical radial distribution feeder. Due to the long transmission distance from the generation units to load points, this type of network experiences a poor voltage profile. That is why reactive compensations, such capacitances and synchronous condensers, have been widely used to meet the voltage standards.

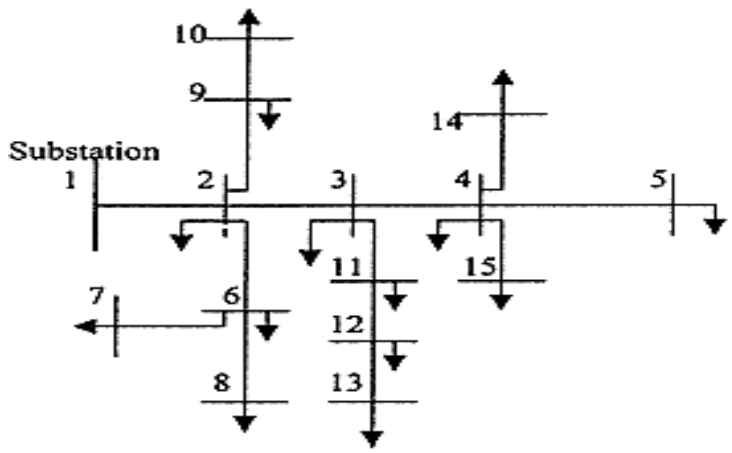

Figure 2.2 Power System Distribution Networks Radial Topology

As it was before, in radial distribution networks there is a single path from the generation units to the down feeders. This is due to the down-stream feeders' passive load which always consumes power. This means that radial networks have an important principal rule called unidirectional power flow which is the same during both normal and faulty working conditions. This rule makes it easy to calculate the fault current level and design an over current protection system using over current relays (R50/51). However, one of the challenges of integrating DGs into these networks is that the unidirectional path for power may change either in steady state or during fault. Integrating DGs changes the passive nature down-stream feeders to an active feeder. After integration, the feeder and its load may need less power or no power and even may inject power into the system. This is a significant change that influences all of the protection system devices and makes their design inapplicable. DGs' integration in radial networks has many impacts; these have been covered in Chapter 3 of this document.

2.3 Power System Protection

Protection system in a power network consists of equipment ensuring the electrical flow reliability and security, and also maintaining the safety of humans and devices. One of the special protection schemes which has been widely used, particularly in distribution networks, is over current protection. Over current protection systems sense the current in various specified grids to avoid exceeding the maximum allowed rate. This goal has been fulfilled mostly by utilizing instantaneous and overcurrent relays (R50/51) and directional overcurrent relays (R67). Relays follow their central logic when tracking the current, sensed by current transformers, in order to determine the proper time for tripping the circuit breaker after fault diagnosis. Many standards, such as IEC 60255 regulate the best function for OCR (Over Current Relays) relays for trip time determinations.

This thesis has a special focus on over current protection as a widely used protection system in high voltage distribution networks. MATLAB has been used for simulating the test cases and benchmarks but it does not include protection devices such as the R50/51 and R61. These are necessary components for an overcurrent protection system design. The design of overcurrent protection has been thoroughly explained in the next section along with design instances for IEEE test cases in order to evaluate DGs integration's multiple impacts. One of the biggest issues in DGs

integration is not losing the system reliability and security. That is, protection system performance should be maintained either by improving and updating it or by applying fundamental reforms.

2.3.1 Over Current Relay R 50/51 and R67

Over Current Relay (OCR) is the most affordable, applicable, and traditional protective element which has been used in radial feeders, particularly in high voltage distribution networks. A typical distribution feeder consists of sets of coordinated over current relays cooperating with automated switches, circuit breakers and possibly recolsers and fuses, depending on voltage level. However, integrating DGs with these networks would affect the protection scheme performance in different aspects. These can be malfunctioning, bad coordination, or even redundancy. As mentioned before, MATLAB does not include protective relays elements. Therefore, in this section the simulated relays 50/51 and their details are presented.

The over current relays are categorized depending on their characteristics into three groups: 1. Definite Current or Instantaneous 2. Definite Time (DT) and 3. Inverse Definite Minimum Time (IDMT). The Overcurrent protection scheme design starts from end downstream feeder to maintain selectivity and also minimum coordination between relays. Using definite time OCRs result in an accumulative large trip time in upstream feeders. However, this is contradictory to those feeders facing a higher fault current, making definite time relays obsolete. Current industrial digital relays such as the SEL-551 are implementing complicated characteristics besides their extra embedded functionalities. IDMT over current relay characteristics fall into some standard styles. IEC 60255 and IEEE define standard curves for IDMT overcurrent relays based on α and β coefficients. General equation describing these curves can be expressed as [2]:

$$\mathrm{T}(\mathrm{I_{sh}}) = \mathrm{TSM} \times \left(\left(\frac{\beta}{\mathrm{PSM}^{\alpha}-1}\right) + \mathrm{M}\right) \tag{2-1}$$

While α, β and M are the relay curve deterministic coefficients, PSM (Plug Setting Multiplier) is the ratio of fault current to pick-up current ($\frac{I_f}{I_{pickup}}$), which is the maximum tolerable current inside the equipment's thermal and electrical limits. TSM (Time Setting Multiplier) is a discrete multiplier which, in recent numerical relays, can be in 0.05 or 0.1 intervals.

α and β should be equal to 0.02 and 0.14, respectively, in order to represent standard inverse OCRs (R51). The OCR 51 with the normal inverse characteristic has been simulated in MATLAB. Figure 2.3 shows the designed relay response signals for a test fault with its calculated RMS current that is depicted in Figure 2.3a. Figure 2.3b illustrates the relay's core function raw output regarding the measured rms current for the test fault that happened at t=0.1 sec. The relay algorithm for fault detection and Trip Time (TT) calculation consists of five logical steps that are shown in Figure 2.3c. The relay's first logical phase shows a clear time when no faults are detected. On the other hand, phase II is related to the fault time transient cycles which can last from 3 to 8 cycles [3]. Output TT should not be calculated based on a fault transient, however it is not recommended to simply ignore transient current since exceeding transients can be very destructive for some equipment. The relay TT is determined based on the transients' maximum. This is being held for 5 cycles to ensure damping transients. After these 5 cycles' minimum time policy, the relay goes into III which is steady state fault current determination. Then the relay is constantly looking for new faults to reduce the determined TT time which is in phase IV. In the last phase, the circuit breaker is commanded to trip and shows that this relay has already reached the promised time. Then the relay stops its processes and just shows the exact time in which the trip command occurred [3].

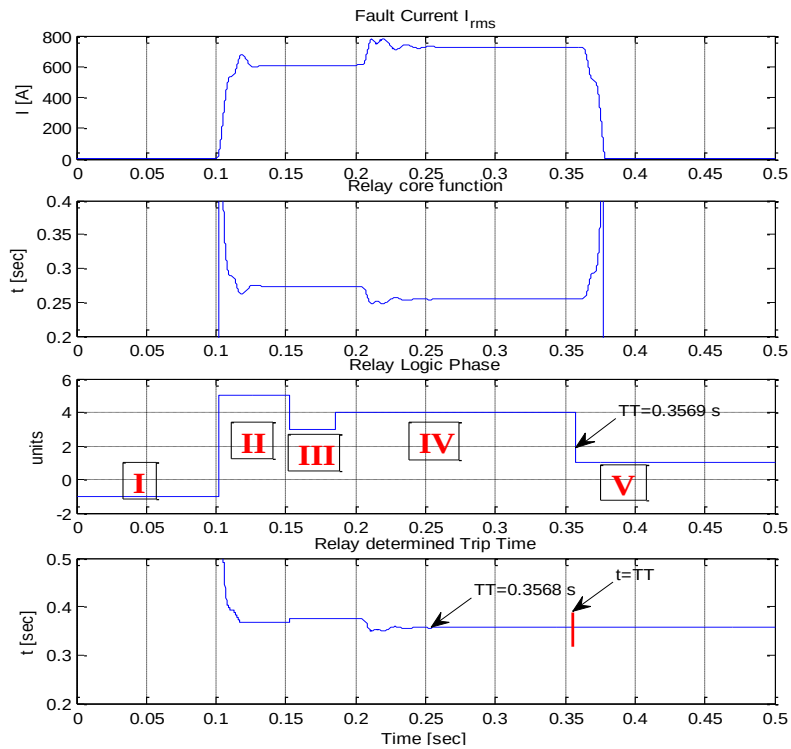

Figure 2.3 OCR 51 Details MATLAB Signal

The same design scheme has been followed in this part to achieve a Directional Overcurrent Relay (R67), but for enhancing the relay capabilities PMU sequence signals have been considered in fault type detection. Results in Figures 2.4 and 2.5 are illustrating the final signal outputs from the designed relay block in MATLAB Simulink. A positive signal sign represent a forward fault and a negative sign is realted to a reverse fault. Then the amount of signal stands for the type of fault as have shown in figures. Both R50/51 and R67 have been simulated in MATLAB Simulink using the embedded coding which runs in each Simulink time step iterations. It should be mentioned that fault type capability has been obtained by using the designed PMU (will be discussed in chapter 4) output sequences' signals.

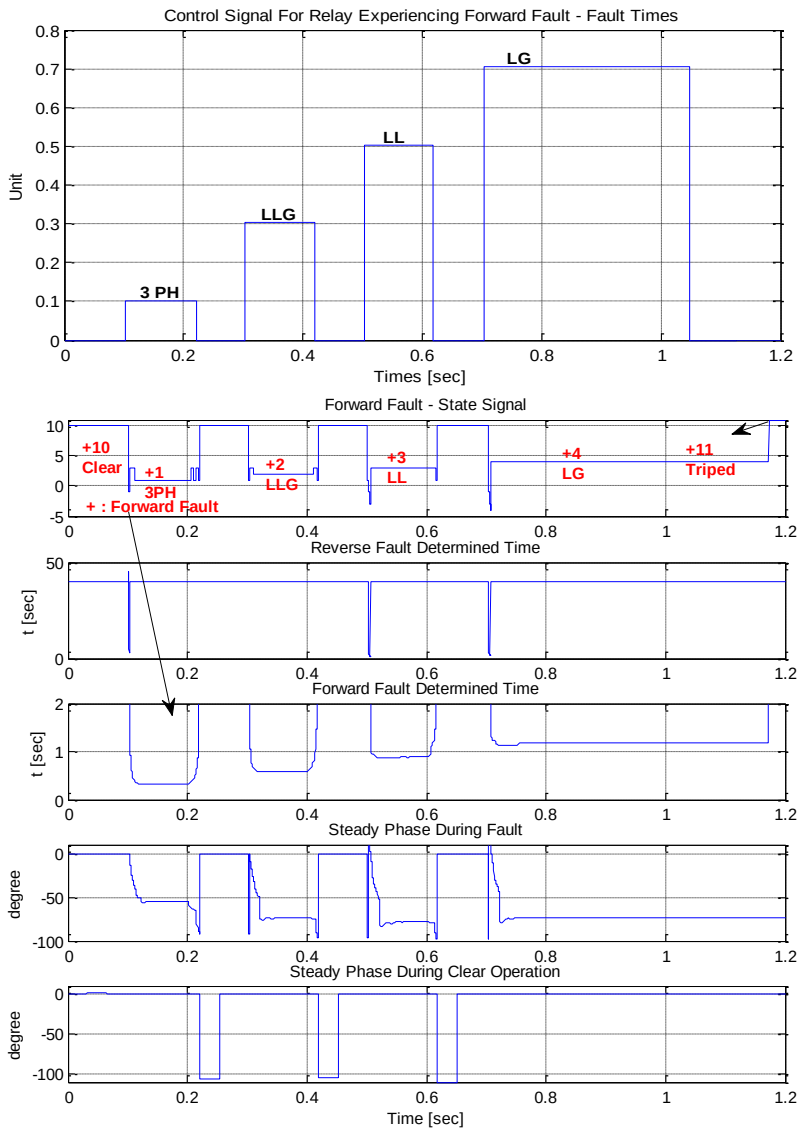

Figure 2.4 DOCR 67 Details MATLAB Signal

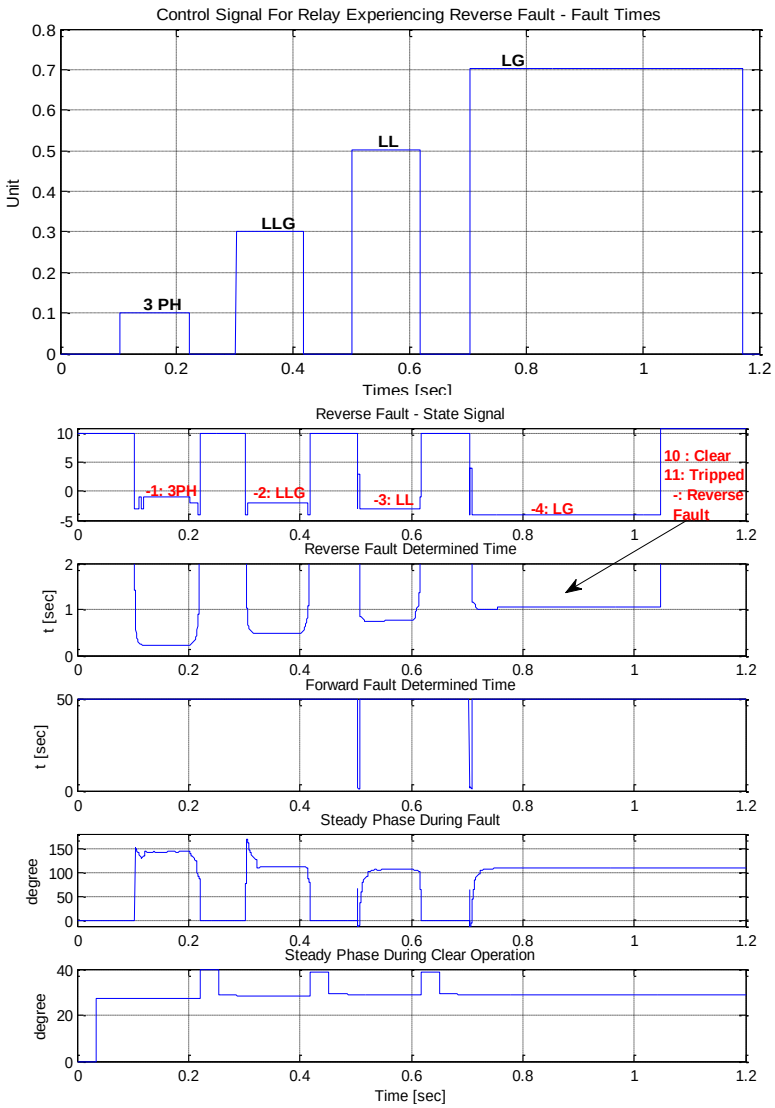

Figure 2.5 DOCR 67 Details MATLAB Signal

2.4 Distributed Generation (DG)

Distributed Generation (DG) is referring to the relatively small and distributed power generation units which mostly take advantage of renewable energies. Different standards and various literatures have proposed controversial and not unified definition for this term. It can be loosely defined as small-scale generator working as a local generation plant for assisting Utility Grids (UG). In addition to generating the electricity and assisting the UG, DGs have more advantages for power systems. Integrating the DGs raises many issues and challenges which, despite their benefits, might threaten the system's security and reliability. That is why world power system leaders decided to go through fundamental changes and improvements in power systems to be able to adaptively accept the DGs with minimum risk. A recently

developed term, Sustainable Energy Resources (SER), also refers to DGs with more emphasis on their renewable energy origination.

DGs integration in power systems is accompanied with many advantages and disadvantages. One of the primary advantages of DGs integration is reducing the path for transmitting the electricity. This reduction results in reducing power loss, improving the voltage profile, decreasing the need for reactive compensation, and also reducing the need for transmission line. On the other hand, some environmental issues also will be resolved by using DGs, which work by renewable resources. The following is a list of some of these advantages:

- Stop transferring electricity
  - Transmission Line Losses
  - Right of Way
  - Congestion
- Quit using Fossil Based Fuels
  - Dependence on Oil
  - Global Warming
  - Carbon Dioxide
- Reduce plants capital investment
  - Private and Public Investment
  - Utility-Costumer Partnership
  - Improving Power Market

DG units take advantage of many energy resources to produce electric energy. This is one of the ways to categorize the DGs based on their natural energy resource. This can be a Fuel Cell, Photo Voltaic, Wind Turbine, Synchronous generator and so on.

Different DGs with various natural energy resources possess special characteristics and may demand different interconnection devices. As a consequence, these differences will lead into different models for different DGs. Four types of DGs have been used in this research work to model and integrate into the benchmarks for constructing interested test cases and scenarios. Wind Turbine, Fuel Cell, Photo Voltaic and synchronous generator are currently some of the most popular and available DGs. Therefore, these four DGs have been chosen to be modeled and integrated into the IEEE test cases for studying protection issues.

2.4.1 Wind Turbines

Wind turbines compose a large share of current DG technology. This is due to its clean energy generation. The first generation of industrial wind turbines synchronous generators has been heavily used. This relatively old type of wind turbines called fixed speed wind turbine utilizes gear boxes to be able to operate in synchronous speed. The gear box increases the wind speed range that the turbine can operate within only trivially, but brings maintenance expenses and risks. However induction generators have fixed this issue. The most famous wind turbines taking advantage of induction generators are called Doubly-Fed Induction Generation (DFIG). Figure 2.6 illustrates a schematic of DFIG and its interconnection. DFIG state space equations are shown in equations 2.2-2.4 [4, 5]:

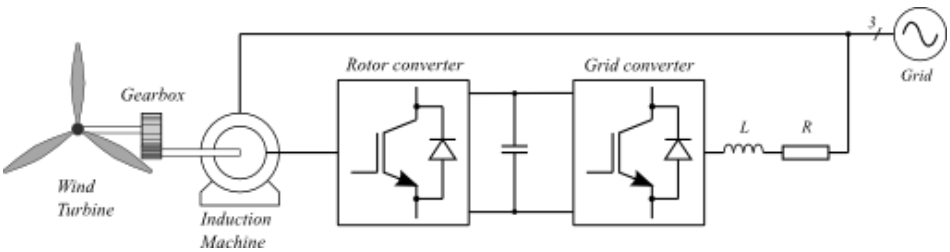

Figure 2.6 DFIG Wind Turbine

$$\begin{bmatrix} u_{ds} \\ u_{qs} \\ u_{dr} \\ u_{qr} \end{bmatrix} = \begin{bmatrix} -R_s - L_s p & L_s & L_m p & -\omega_e L_m \\ -\omega_e L_s & -R_s - L_s p & \omega_e L_m & L_m p \\ -L_m p & (\omega_e - \omega_g) L_m & R_r + L_r p & -(\omega_e - \omega_g) L_r \\ -(\omega_e - \omega_g) L_m & -L_m p & (\omega_e - \omega_g) L_r & R_r + L_r p \end{bmatrix} \begin{bmatrix} i_{ds} \\ i_{qs} \\ i_{dr} \\ i_{qr} \end{bmatrix} \tag{2.2}$$

$$T_e = L_m \left(i_{qs} i_{dr} - i_{ds} i_{qr} \right) \tag{2.3}$$

$$S = \omega_e - \omega_g \tag{2.4}$$

The use of induction generation in DFIG allows them to work with a large range of wind speeds. A back-to-back voltage controlled power electronic interface feeds the DFIG wound rotor in order to control the excitation current magnitude and frequency. This interface, which has a significant role in DFIG operation, consists of an AC to DC rectifier in the grid side which is also called grid side converter, and a DC to AC inverter, which is also called rotor side converter. These two power electronic converters use control algorithms to evaluate the d-q axis required in the induction motor wound rotor to reach the pre-defined frequency and voltage output. Using this technique and by manipulating the rotor current and frequency the induction generation can operate within a wide range of wind speed (5 to 25 m/s). On the other hand, these back-to-back converters are able to regulate the output power. This is how the DFIG can produce desired output feedbacks such as output active power, reactive power, calculating the variations and current d-q axis. Therefore DFIG and some other DGs which will be connected to the network using such a power electronic interface have the ability to regulate their reactive output power as long as it is within its nominal rating. Besides assisting UG in reactive power production, DGs are also able to produce reactive power and relieve the distribution networks from reactive compensations and capacitors. However, these interfaces have their own impacts and limitations. IEEE 1547 regulates all types of DG interconnections in regards to meeting various standards including power quality, harmonics, power protection and fault condition response. Power electronic interfaces can inject a significant amount of harmonics into the system.

2.4.2 Fuel Cell (FC)

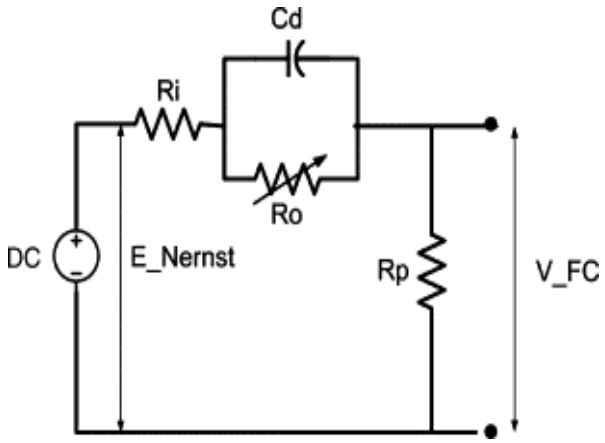

Figure 2.7 FC Electrical Equivalent

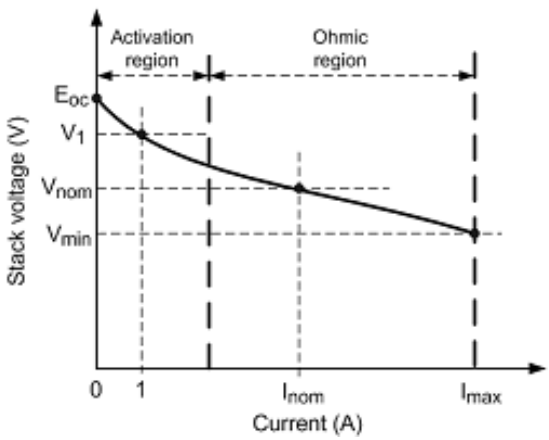

Figure 2.8 FC Characteristic Curve

Fuel Cells are one the most innovative recently well-developed DG types. In this thesis, the Proton Exchange Membrane Fuel Cell (PEMFC) MATLAB modules have been used along with a boost converter and an IGBT inverter with suitable output filters and transformers. Figures 2.7 and 2.8 depict a FC electrical model and characteristics curve. The FC is a DC power generator; therefore, it needs a power inverter. This is the reason that FC is also categorized as power electronic interfaced DG. In the following subsection a discussion regarding the different types of FCs will be made.

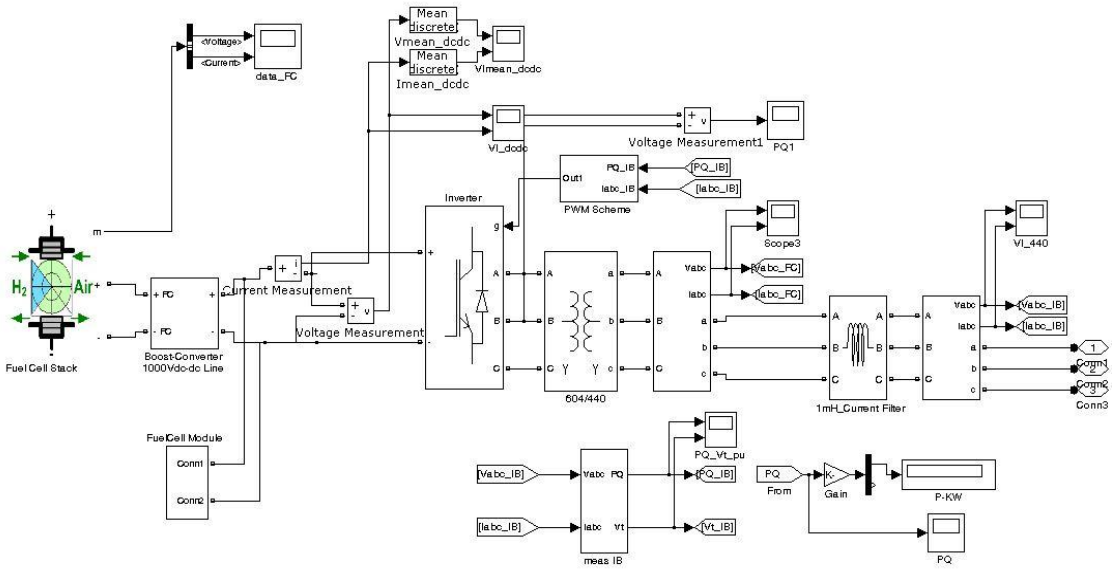

Figure 2.9 FC MATLAB Model

2.4.3 Photo Voltaic (PV)

Photo Voltaic (PV) DG modeled using MATLAB based on the Figures 2.10 and 2.11 depicts that PV electrical equivalent circuit and PV characteristics curve. Figure 2.12 shows the MATLAB block diagram modeled for PV. The SunPower SPR-305-WHT PV cell with 5 series cells and using 350 parallel strings has been used to reach preferred voltage. Since PV, like FC, is a DC generation unit, a DG a boost converter has been used to provide the inverter with a constant DC link. A voltage controlled inverter has been used to invert the DC current to AC with defined frequency.

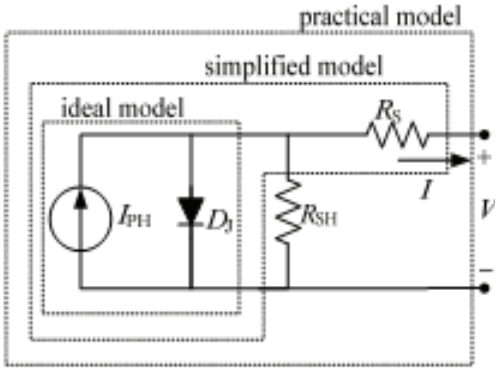

Figure 2.10 PV Electrical Equivalent

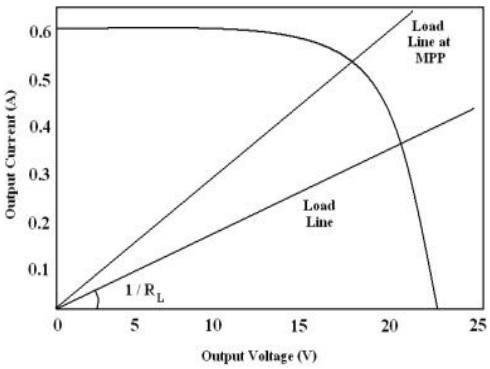

Figure 2.11 PV Characteristic Curve

2.4.4 Synchronous Generator

Synchronous generators with small and medium ratings are also being used for DGs. Some turbines such as the Aeroderivative gas turbines and many other types of synchronous generators are currently working in industries, harbors, and hospitals as back up or emergency units that can be employed as DGs once the infrastructure is ready to integrate them. However, the reason that we are using a synchronous generator is so that it can serve as an example of DGs that do not need any interconnection to be coupled with power systems. Synchronous DGs take advantage of AVR and Governor to control their output voltage and active power as well as frequency and reactive power. This makes a significant difference in these types of DGs' response during power system disturbances, particularly during severe faults. This will be explained in more detail in the next section.

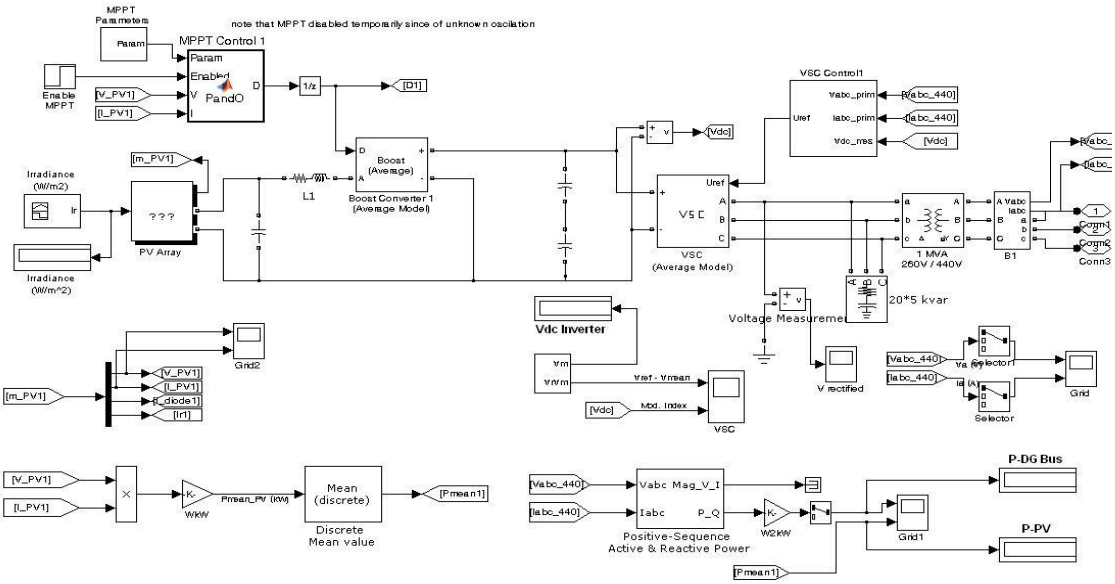

Figure 2.12 PV MATLAB Model

2.5 DGs Interconnections

Different DGs use different interconnections to be coupled to power systems, as has been briefly discussed in previous section. DGs fall into two groups based on their interconnections:

- Directly Interfaced Distribution Generators (DIDG)
- Inverter Interfaced Distributed Generators (IIDG)

DGs' interconnection plays a critical role in investigating system protection issues after their integration. The first group, DIDG, is connected to the network directly. DGs such as fixed speed wind turbines, micro turbines, small synchronous turbines and Aeroderivative gas turbines are examples of systems which fall within this category. DIDG DGs have their own systems to be regulated in case of output voltage and frequency as their first priority and also to produce the desired active and reactive power. That is, DIDG do not use any power electronic based interconnection since their produced electricity is not DC originated. Therefore in case of fault or disturbances, DIDGs' responses are more similar to ordinary power generation units, but in smaller scales. A gas or steam power generation unit or any other rotatory machine has a fault current between 5 to 13 times their nominal current. This originates from the electromagnetic field stored in the rotatory machine iron which can be released quickly to produce excessive current. Also, the machine torque has the ability to support it in case of fault. The IIDG group refers to the DGs which need some power electronic devices to connect to the power systems. DGs whose power originated from a DC source are good examples of this. Recently developed DGs

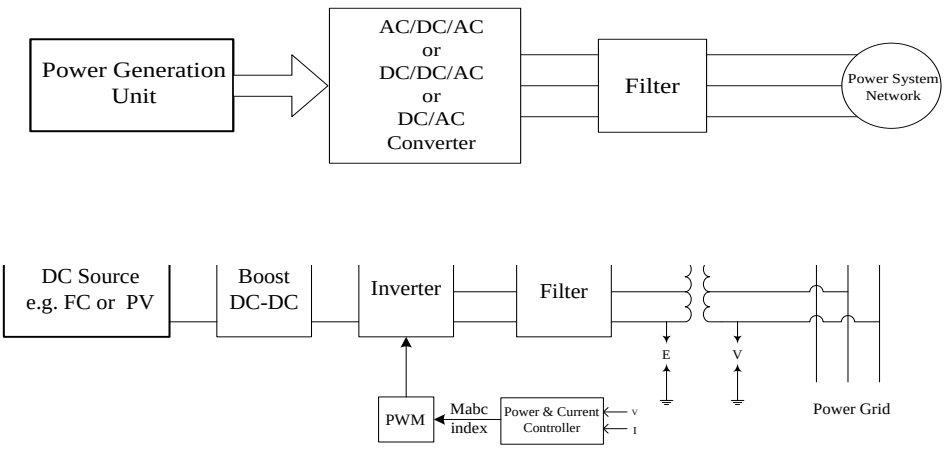

Figure 2.13a) IIDG Scheme, b) DC Base IIDG Power Grid Interface

which take advantage of various renewable and sustainable energy resources do not necessarily meet the requirements and regulations. For this reason, they need power electronic interconnections to regulate their DC produced power in desired AC with proper voltage and frequency. Figure 2.13 shows some of the most typical structures for such interconnections. There are many schemes that are applicable for connecting DGs to the network. Figure 2.13.b depicts the most typical and industrial version for DC based sources. In this interconnection, the source produced DC current will change into a preferable voltage level by a boost converter. The boost converter increases the voltage level of the small voltage generated, maintaining a theoretically and mostly stable constant DC link for the inverter by using a capacitance in its link to an inverter. At last the inverter produces the AC power using the constant provided DC even during a fault or any other transients. The inverter output will be smoothened by an output filter for harmonic reduction. One the advantages of using this inverter interface is that we can demand a DG unit to produce reactive power using its power electronic switches just as a FACTS device. However, a power electronic interface has its own limits and boundaries such maximum current. Typically, manufacturers utilize their own protection scheme to protect the inverter section and its switches against over current, over voltage, and spikes. Therefore, an IIDG generation unit does not contribute to fault current compared to the DIDG DG. Manufacturers' protection schemes normally limit the inverter current by setting their control and protection setting to 100%-400% of their nominal current. Therefore, during fault an IIDG unit does not contribute to the fault current as it was expected. This is an important piece of information which should be considered both in integrating DGs and also regulating the networks' protection for DGs' employment. For instance, a DFIG generation unit, even though it is a rotatory generation unit, does not contribute in a fault like a synchronous generator. DFIG, PV, and FC control setting in their power electronic devices limits the current from exceeding the switches maximum allowed rate. Although some prototypes may have a transient significant current between 4 to 6 times of their fault steady state current, this transient will be mitigated in less than 3 cycles, usually in the first cycle.

Figures 2.14 to 2.16 illustrate the discussed issue for DGs that has been simulated in this work. All DGs have been exposed to a faulty scenario when each fault stays for 0.2 seconds and a 0.2 seconds intermittent have been given between faults so DGs are able to restore. The first fault is a balanced bolted 3-ph fault and after 0.4 seconds the system will experience a LLG fault. At the end a LG fault will be also tested on the system to investigate all fault types for comparing their resulted currents. Figure 2.14 depicts the synchronous generator fault response. From this figure it can be seen that the synchronous DGs will highly contribute to the fault current as it has been discussed before. This contribution can be between 5 to 13 fold of their rating current and will be ended only by protective relays such as OCR 50/51.

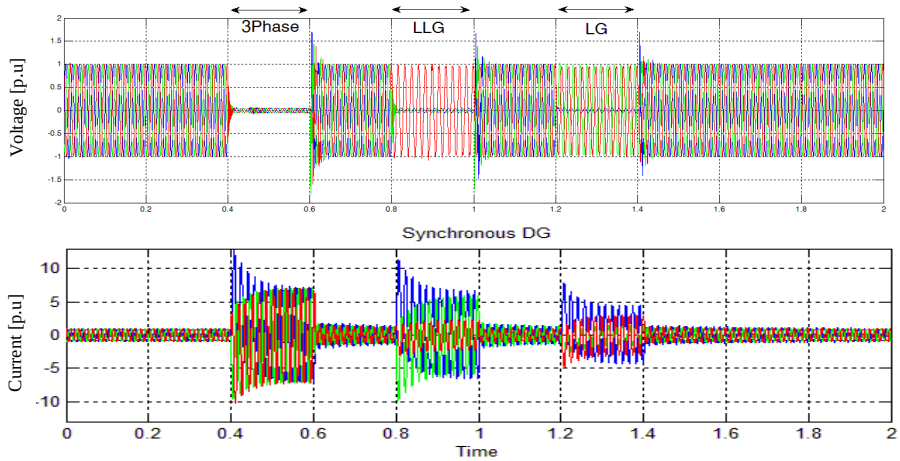

Figure 2.14 Synchronous Generator Responses to Various Fault Scenarios

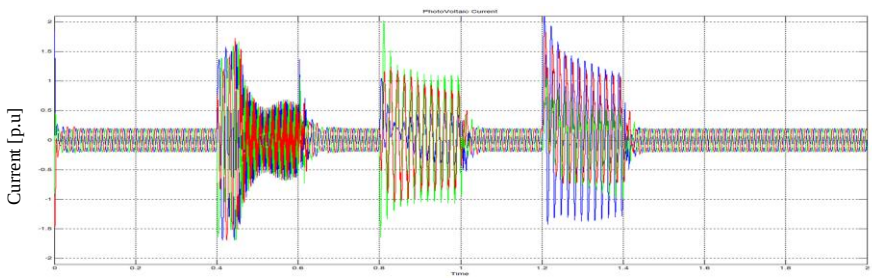

Figure 2.15 PV Responses to Various Fault Scenarios

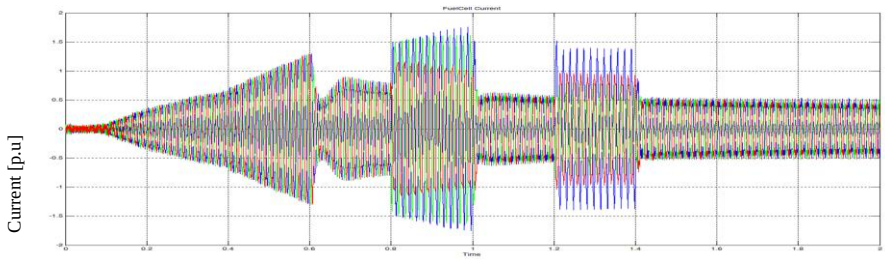

Figure 2.16 FC Responses to Various Fault Scenarios

Chapter Three
DGs Integration Impacts

3.1 Overview

Installing Distributed Generators (DG) in distribution networks brings many advantages such as improving voltage, power quality, mitigating voltage sags, improving transmission system congestion, and providing more affordable capacity for utilizing renewable energy resources. All of these factors lead utility companies to integrate DGs into current distribution networks as much as possible. This integration benefits both the customer and utility sides. However, this incorporation will change the radial distribution networks' fundamental aspects: upstream or Utility Grid (UG) feeding, passive feeders and fault current path. The network protection system has been designed based on old traditional fundamentals and unable to adapt with new changes. Over current protection, switchgears, and circuit breakers all have been designed, chosen, and set based on passive down-stream feeders with constant amounts of current for different scenarios.

Therefore, suitable measures should be taken before this integration to avoid the loss of system reliability and security. This section investigates the consequences of DG integration into the current distribution networks, such as bus voltage profile, fault current level, and contribution. The DGs' integration impacts have been categorized in this study after their evaluation based on system operation. Two IEEE recommendations have been chosen as test cases for studying DG integration. IEEE 13-bus HV industrial distribution network and IEEE 34-Bus unbalanced network have been simulated in details using MATLAB SimPowerSys. Four different types of DGs have been employed in three scenarios with different penetration levels. Different DG types enable us to investigate the DG interconnection impacts on fault current characteristics and sharing. Besides the simple integration, we would be able to evaluate the DGs penetration impacts on discovered issues. On the other hand, as it has been discussed, one DIDG and three IIDG have been chosen in order to evaluate and prove the impacts of the DGs' interconnection

.

3.2 Impacts on Power System

3.2.1 Structure Alteration

According to the recent research and studies, distributed generation is universally accepted as an effective and economic solution to answer the ever increasing power system demands [5]. It's been decided by the United States' Department of Energy (DOE) and Distributed Energy office (DE) that 22% of new installed generation capacity should be from DGs by the year 2012. This is why DG is considered a major option to ease most of the current network problems such as power loss, power consumption demand, voltage quality, line congestion, security, and reliability. Also, this approach leads toward reaching the goal of easily utilizing green and renewable energy resources in case of global carbon-dioxide production reduction.

Current Distribution Networks are generally designed in a simple radial scheme, that is traditionally fed from upstream Utility Grid (UG) sides through LV and passive downstream feeders [5, 6]. Thus, in radial networks we have a unidirectional power flow and a same-directed current from UG towards downstream feeders, which makes it easy to calculate the fault current level completely provided by the UG connection. Therefore, design a protection scheme is easier in radial network comparing too loop networks [7]. On the other hand, buses voltage level decreases by getting farther from the UG connection. That is why radial networks have a poor voltage profile which should be corrected by capacitance, synchronous compensators, or FACTS devices at weak points. Adding DGs in such networks improves the voltage profile, but it changes the system's fundamental characteristics and network impedance. Power

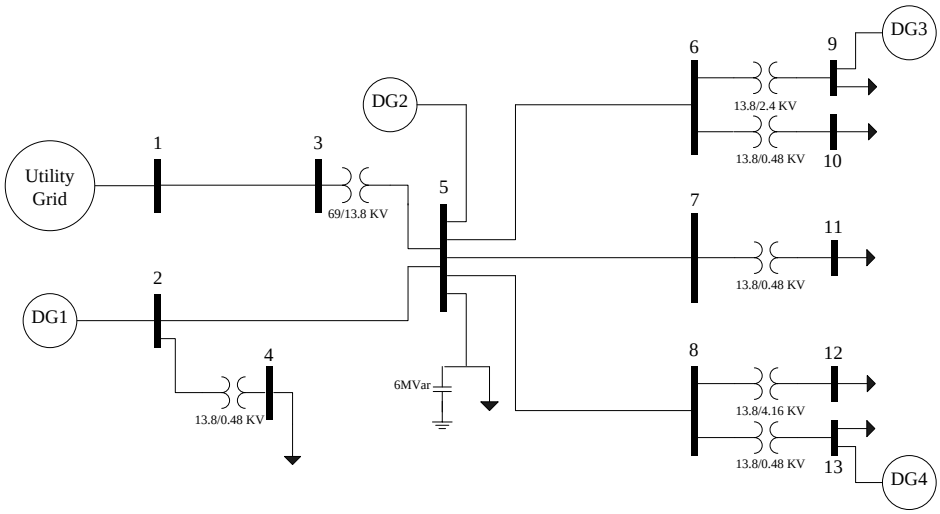

Figure 3.1 IEEE 13-Bus Radial Distribution System

Table 3.1 Bus P-Q Values for IEEE 13-Bus

Bus Number	Active Power[KW]	Reactive Power[KVar]
4	600	530
5	2240	2000
9	2800	2500
10	370	330
11	810	800
12	1310	1130
13	1150	290

system admittance, as a critical characteristic of the system, determines many system traits. Many system designs have been processed based on this important matrix. Integrating DGs into the network adds parallel impedances with power system matrices per each DG installed on each bus. However, figuring the IIDG equivalent impedance is so controversial that there is a lot of literature which proposes various schemes for it. By considering it, one can supervise and predict the consequences of such a critical change in a network's fundamental factor.

Besides all of the advantages DG provides for power systems, there are some complexities which it brings for networks, especially those planned with old and traditional topologies. Hence, different types of DG integration effects should be investigated in order to avoid losing network security and reliability. Suitable measures should be taken to adapt the network by regulating devices and proposing new algorithms and considering currently installed elements.

3.2.2 Voltage Profile

In this section an IEEE 13-Bus industrial radial distribution network is used to carry out simulation results using MATLAB/Simulink in order to investigate DG integration impacts. The system was extracted from a common medium-sized industrial plant which has been used for many examples and calculations in IEEE Color Books series [7, 8]. The system feeds from a 69 KV utility grid that is assumed to have a strong bus connection. Bus load values can be found in table 3.1. Figure 3.1 shows 13-Bus system integrated with one DIDG (synchronous) and three IIDGs (FC, PV and DFIG). DG

buses are allocated using 2/3 rule in order to obtain a fair power loss and voltage impact [9]. Besides the original system, two case studies with different DG penetrations are simulated in normal and varied faulty condition to acquire a clear result how DG affects the system. DG power capacity details can be found in table 1 along with case study details.

The nature of radial distribution networks is to feed downstream feeders from a single UG connection. Transferring power through long lines, passing of different transformers, loads, and the other power electrical elements cause significant voltage reduction due to series components impedances. In traditional networks, voltage profile is usually improved by adding capacitors, synchronous compensators, or FACTS devices. Scattering distributed generators in such networks reduces the amount of transferred power, while suitable allocation and penetration must be considered [9]. Subsequently, reducing system power loss leads to obtaining better voltage supply, particularly regarding downstream feeders' endpoints during full load time. These consequences would be more important and critical in fault conditions.

Distribution transmission lines usually feed uniform loads. Hence transferred power in a distribution line point k can be expressed as a function of its length and distance from generation point. If *0* denotes the UG connection point and *l* is the line's last point of load feeding, the transferred power can be expressed as bellow:

$$\begin{cases} P_{0-d} = \frac{d}{l} P_l \, , P_{d-l} = \left(1 - \frac{d}{l}\right) P_l \\ Q_{0-d} = \frac{d}{l} Q_l \, , Q_{d-l} = \left(1 - \frac{d}{l}\right) Q_l \end{cases} \tag{3.1}$$

Table 3.2 Case Studies

DG Penetration in Case #	Active Power Production [MW]			
	Utility Grid	DGs sum	DG share	DG# & Type
Case1 (base case)	9.2	0	N/A	N/A
Case 2 (40%)	5.7	3.5	2	1-Syn
			0.5	2-DFIG
			0.5	3-PV
			0.5	4-FC
Case 3 (90%)	0.7	9	4	1-Syn
			2	2-DFIG
			2	3-PV
			1	4-FC

Voltage of any point of the transmission line as well as buses can be calculated based on the DG position within the line (denoted as k). If the initial point of the line would have u_0 voltage, then:

$$u_0 = u_0 - \Delta U = u_0 - \Delta U_1 - \Delta U_2 \tag{3.2}$$

As ΔU is the voltage drop, ΔU_1 caused from the initial point to the point of DG installation and ΔU_2happens from the DG installation point (k) to the end of the line. Two cases are as follow:

Case 1: $0 < d \leq k$ (point *d* before DG)

$$\Delta U_1 = d\frac{rP_{d-l}+xQ_{d-l}}{u_N} \tag{3.3}$$

$$\Delta U_2 = \frac{d}{2}\frac{rP_{0-d}+xQ_{0-d}}{u_N} \tag{3.4}$$

$$u_d = u_0 - \frac{d}{u_N}\left[\left(1-\frac{d}{2l}\right)(rP_l + xQ_l) - (rP_{DG} + xQ_{DG})\right] \tag{3.5}$$

Case 2: $k < d \leq l$ (point *d* after DG)

With the same method in case one, point d voltage will be:

$$u_d = u_0 - \frac{d}{u_N}\left(1-\frac{d}{2l}\right)(rP_l + xQ_l) + (\frac{rkP_{DG}+xkQ_{DG}}{u_N}) \tag{3.6}$$

The formulas above refer to the fact that DGs integration improves network voltage profile proportional to their active and reactive capacity. Figure 3.2 depicts a typical radial distribution feeder poor voltage profile which is a characteristic for those types

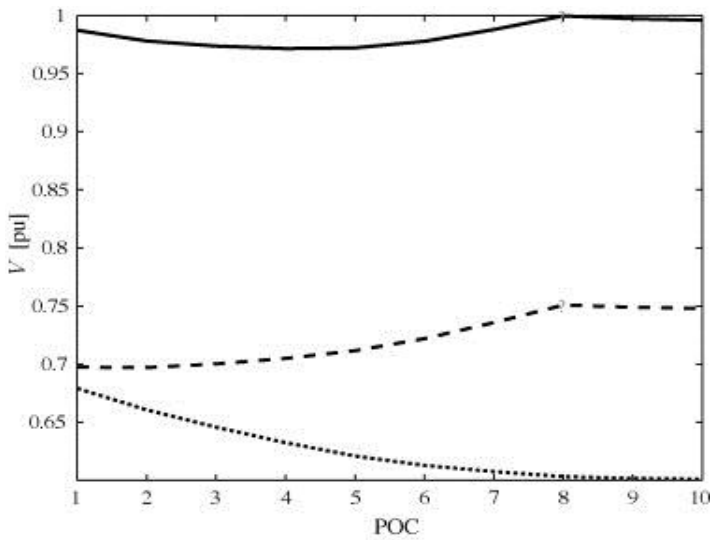

Figure 3.2 A Typical Radial Distribution Feeder Voltage Profile

of network structures. Power system engineers used to improve these declining profiles by installing capacitive compensations or other expensive and more complicated compensators based on the network voltage level and priority. DGs resulting compensation causes voltage recover in bus 8 as it has been shown in the plot below. Figure 3.3 illustrates system voltage profiles of three case studies. It is clear from the base case graph that using a transformer taps the minimum voltage decreased to less than 0.97 per unit. Meanwhile, in case 2 with DGs integration, voltages improved at least 1% at any buses. In case 3 we have a desired voltage magnitude in most buses while there are 3 buses with roughly 1% excessive voltage that originates from constant transformer taps in different cases. This can be easily fixed in a practical industrial network. It should be mentioned that transformers tap have been extracted from recommended IEEE 13-Bus test case and remains constant after adding DGs to the network. Hence DGs incorporation impacts over the test case can be watched in the situation where no precautionary step has been taken. Mechanical and automatic Tap Changer Transformers are one of the conventional ways that utility companies use along with capacitive compensation to avoid voltage dropping less than allowed rates. However it is beyond a doubt that these types of compensations have many disadvantages.

Different faults have been used at different buses in order to investigate system voltage profiles and stability during fault condition. Some DGs have a protection scheme to shut down the unit or enter island mode, but voltage stability during fault is a vital concern for any network during any period, i.e. load voltages, neighbor regions' voltage stability, relays and protection device accuracy. It has been proven that power

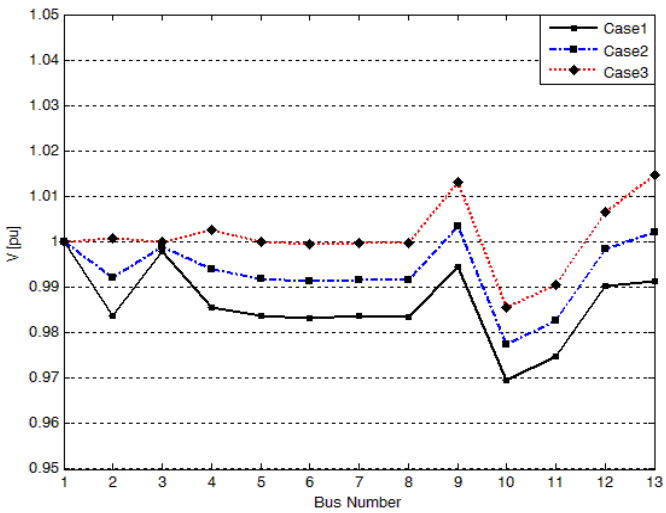

Figure 3.3 IEEE 13-Bus Voltage Profile

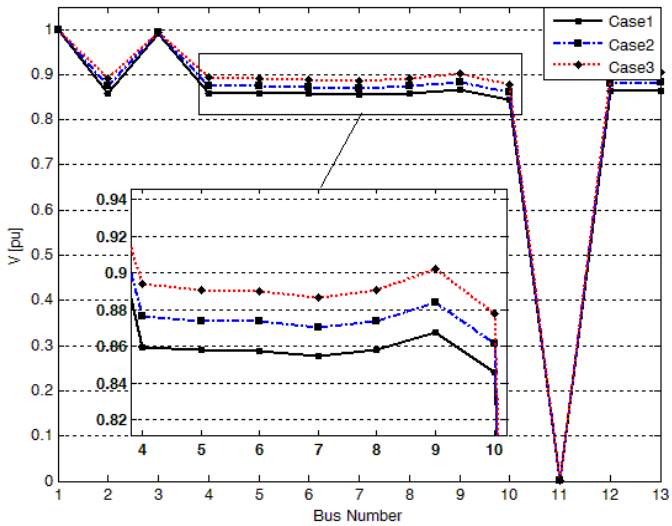

Figure 3.4 System Voltage Profile with Fault at Bus 11

systems which are able to maintain a higher voltage level during sever faults are less likely to experience a relay, breaker, or switchgear malfunction. On the other hand, by maintaining voltage within the fault current during fault, it is easier for digital relays to detect the instrumentation (current/voltage) transformers saturations. Figure 3.4 illustrates system voltage profiles after fault current threshold damping for a bolted 3-ph fault occurred at bus 11 in IEEE 13-Bus test case simulated using MATLAB's power system toolbox. It is clear from plot magnifier that DG integration adds approximately 2 % improvement at all severely-affected bus. For instance, we have 0.844 p.u voltage at bus 10 (PQ) which was increased to 0.879 p.u; nearly a 4 % improvement in case 3. As it has been shown, the black curve refers to the base case (case 1) which is the system without any integrated DGs and the dotted blue and red curves are related to case 2 and 3 with 40% and 90% DGs penetrations respectively.

3.2.3 Fault Current Level

Fault situation is an important issue in DGs integration. It is clear from the previous section that DG integration improves voltage profile. However, as mentioned before, adding DGs into power networks alters the system impedance matrix, i.e. bus Thevenin impedance reduction [9]. Those two major impacts yield a fault current increase in the power network which drastically influences system security and reliability due to loss protection devices accuracy or response. Although there are discriminations between IIDG and DIDG generations but even IIDG limited fault current along with UG and rest of DIDGs' share impresses protection system. Figure 3.5 shows a simple radial power network during 3 phase bolted fault with a DG integrated in the system. In figure 3.6, a and b show the equivalent circuits for the

radial networks DG added in Figure 3.5. Defining mesh currents I_1 and I_2 from 5.a and applying the Kirchhoff law results in the equation below, yielding currents:

$$\begin{bmatrix} U_s \\ U_g \end{bmatrix} = \begin{bmatrix} Z_s + Z_L & (1-l).Z_L \\ (1-l).Z_L & Z_g + (1-l).Z_L \end{bmatrix} \begin{bmatrix} I_1 \\ I_2 \end{bmatrix} \tag{3.7}$$

$$Z_{th} = \frac{(Z_s + l.Z_L).Z_g}{(Z_s + l.Z_L) + Z_g} + (1-l).Z_L \tag{3.8}$$

As $l = \frac{p}{d}$, when p is a transmission line impedance from UG to point of DG installation and d is the all line impedance (UG to the fault point). Then equivalent Thevenin circuit yields as 5.b and Thevenin impedance as mentioned. Therefore fault current can be calculated by formula 3.9:

$$I_{f,3ph} = \frac{U_{th}}{\sqrt{3}.Z_{th}} \tag{3.9}$$

By substituting $U_{th}$and Z_{th}in equation 3.9 fault current would be.

$$I_{f,3ph} = \frac{U_{th}.(Z_s + l.Z_L + Z_g)}{\sqrt{3}[(Z_L.Z_g + Z_s.Z_g + Z_s.Z_L) + l.Z_L(Z_L - Z_s) - l^2 {Z_L}^2]} \tag{3.10}$$

Considering the fact that the nominator increases, both by the impedances and voltage profile improvement, fault current level increases as it shown in table 3.2 resulted by simulated cases.

Table 3.3 Fault Current in Blackout for Various Faults

Fault Type	Case #	Faulty Bus				
		B5	B6	B7	B11	B12
3 Phase-Ground	Base Case	17.83	17.48	17.28	2.28	2.54
	Case 2	19.70	18.88	18.70	2.33	2.60
	Case 3	21.22	20.84	20.57	2.37	2.65
Line-Line	Base Case	15.47	15.1	14.98	1.98	2.19
	Case 2	16.86	16.44	16.29	2.01	2.25
	Case 3	18.12	17.32	17.24	2.06	2.30
Line-Ground	Base Case	12.24	11.97	11.09	1.45	1.58
	Case 2	13.05	12.49	12.18	1.46	1.59
	Case 3	14.31	13.36	13.01	1.46	1.60

Considering the source's current contribution based on observing impedances through the fault, UG share in equation 3.10 can be calculated as:

$$I_{f,grid} = \frac{Z_g}{(Z_s + l.Z_L + Z_g)} . I_{f,3ph} \tag{3.11}$$

$$I_{f,grid} = \frac{U_{th}.Z_g}{\sqrt{3}[(Z_L.Z_g + Z_s.Z_g + Z_s.Z_L) + l.Z_L(Z_L - Z_s) - l^2 Z_L{}^2]} \tag{3.12}$$

Simulation results carried out for varied faults at different buses to obtain a more reliable assessment and confirming the above discussion. Table 3.3 shows fault current levels for different faults at some chosen buses. It is clear that DGs integration into the system increased fault current levels with different scales based on fault location. For example in bus 5, which is located quite near to the utility grid, we have 3.37 p.u increases in comparison with base case which is not acceptable without protection system regulation. Also in a load bus, i.e. bus 12, fault current increased by 0.11 p.u which equals to 152.7 in amps. It has been mentioned in the mathematical proof that as far as we are getting from the UG and DGs point of connection, when l is approaching to unity, the amount of increase in fault current rate is more significant. It can be deduced from formula 3.10 which increasing the l decreases the denominator as a result of the square factor with negative sign.

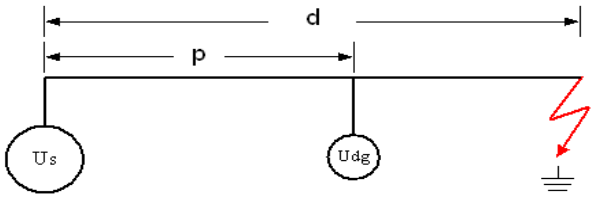

Figure 3.5 DGs Integration in Feeder

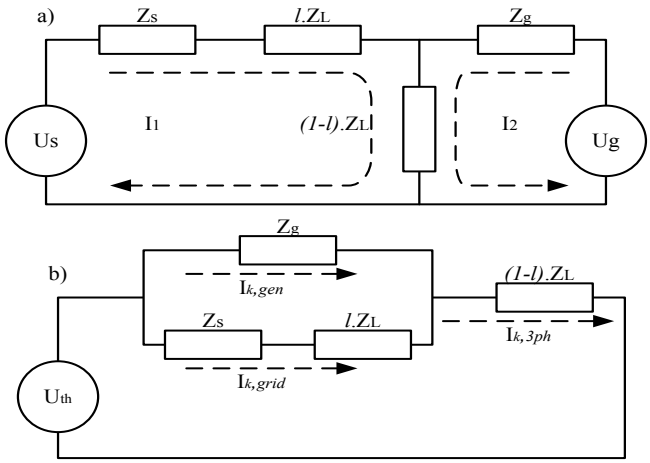

Figure 3.6 a) with Integrated DG b) Equivalent Network

3.2.4 Fault Current Contribution

By adding DGs to the system, utility grids do not see the same impedance during fault as they used to. Therefore, their contribution into the fault current may change by DG locations and capacity. As it is clear in equation 3.12, the amount in change in UG share relies on DGs impact on voltage profile, DGs impedance, and more importantly their location regarding fault and UG location. Figure 3.7 and 3.8 illustrate UG contribution in a solid 3-phase to ground fault, which occurred respectively at bus 12 and 11. It is clear from the plot that utility share of fault current decreased with DG existence in network as we expected. One can deduce from the Figure 3.7 which UG fault current share reduced by 0.8 p.u after adding DG to the system. Also there is a 0.716 p.u reduction in UG fault current share with DG existence which is roughly 24%, as shown in Figure 3.7. This is a critical alteration regarding protection system regulation, particularly if DGs would be decisive to connect to the network and generate power. This ideal network with private DG owners who decide when to connect their generators to the network demands more than a simple protection system regulation, i.e. smart and adaptive protection. On the other it should be mentioned that DGs types have significant impacts on UG fault share change. In fact, DGs with power electronics interconnections usually do not really affect the fault share and UG contribution as a matter of their own protective policies. Some wind turbines, micro turbines, and rotatory small synchronous DGs have a more significant impact on fault share traits.

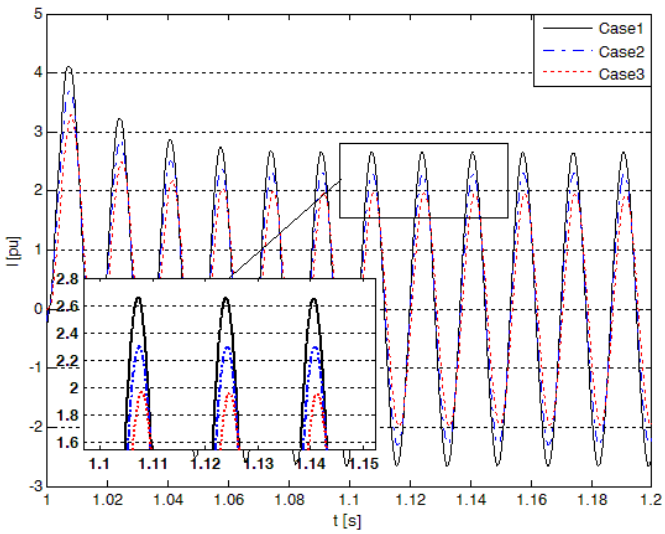

Figure 3.7 UG's Contribution in 3-ph Bolted Fault at Bus 12

3.3 Impacts on Protection System

3.3.1 IEEE 34-Bus and Protection System

Central Protection Unit (CPU) manipulates digital relays adaptively by changing the system structure and DGs matrix. This section has been dedicated for the goal of investigating various effects that DGs integration imposes on a protection system that is already designed and operational, particularly for over-current protection. DGs integration into current networks can be a critical and delicate process. Depending on DG size and penetration, location, type, network interconnection, and structure, it can bring a variety of negative aspects which should be considered in advance. A radial power distribution network is the most common and economical scheme for transferring power to both industrial and residential areas. Ease of design, construction and expansion for such networks accompanies with more demand for DGs integration. However, DGs employment alters the fundamentals which radial networks and their consisting equipment are based on. The major changes in these principles can be categorized as:

- Power Flow
- Voltage Profile
- Admittance Matrix
- Fault Current Characteristics (level, share, and path)

The major protection scheme in radial networks is over current protection system for both primary and back up. Such protection systems can be desperately affected by new network conditions unless proper measures have been taken. The goal of this

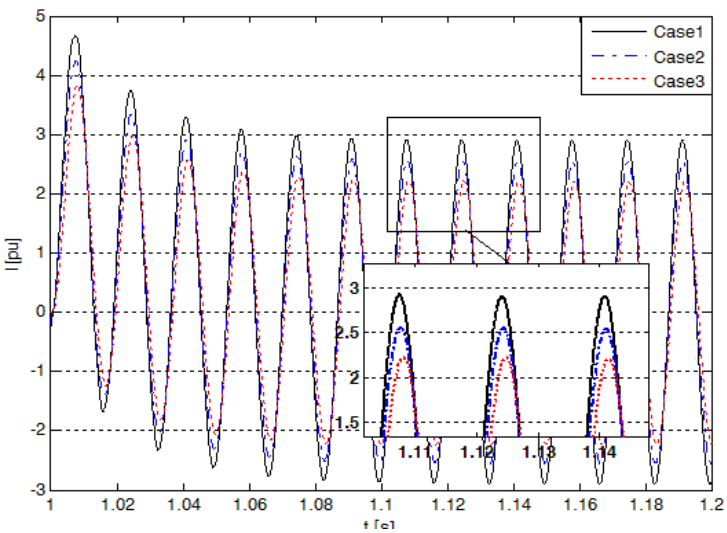

Figure 3.8 UG Contribution in 3-ph Bolted Fault at Bus 11

study is to identify and quantify the impacts of DGs integration into a radial network's protection scheme and subsequently the network's reliability and security. IEEE's distribution feeders subcommittee has published a set of radial distribution networks. Discussion and results in this section were carried out from comprehensive MATLAB simulation on IEEE 34-bus benchmark incorporated with two types of DGs. The over current protection system has been designed using a modeled OCR 50/51 relay which tried to be similar to its industrial counterparts, like SEL-551, though in simpler scale as it has been explained in section 2.3.

The IEEE's distribution feeders subcommittee has published several test cases which are available at [10] including IEEE 34-Bus. The main purpose of these test systems is to evaluate the distribution power network's software performance and accuracy [9, 10]. The IEEE 34-Bus test case which has been chosen in this study is not the largest test case in this category, though it does consist of a good variety of components and elements. However, it also can cause convergence issues originating from its length and unbalanced loads and currents. There are also some compatibility problems for simulating some of its components in software such MATLAB. The original test case consists of two three-phase and five single- and double-phase lateral feeding spots and distributed loads. There are two On-Load Tap Changer Transformer (OLTC) or voltage regulators and also two three phase voltage transformers at buses 800 and 888. Although OLTC with individual changing taps has been simulated by an author in MATLAB Simulink, it has been ignored in studied test cases in order to magnify the effect of DGs integration voltage profile improvement on a protection system's critical areas. Regardless, using designed OLTC severely slows down the simulation processing time, which for such a sophisticated system would be a significant amount of time.

Figure 3.9 shows the modified IEEE 34-Bus test case with DGs integrated into it. The bus names provide both for IEEE test nodes and conventional labeling (separated by /) for radial distributed feeders based on layers. In this bus labeling, which is called branch numbering, the buses which are located in the same circular bus layer far from the utility grid are named first and next layer will be labeled as such in next steps The variety of loads which have been used in the original case are not available in SimPowerSystem simulation tool while has been simulated for reach the most accuracy in results. That is constant current and power (I, PQ) loads besides constant

impedance loads have been simulated. Distributed and spot loads with both D and Y connections have been simulated in this model. All distributed loads are assumed to be located at the end of their related feeders' lines since this does not affect our results. Constant current and PQ loads have been modeled using the static load model which represents the relationship between power and voltage as an exponential usually expressed in following equations:

$$P = P_0 \left(\frac{V}{V_0}\right)^{n_p} \tag{3.13}$$

$$Q = Q_0 \left(\frac{V}{V_0}\right)^{n_q} \tag{3.14}$$

In which n_p is the active power exponent and n_q is the reactive power exponent. P_0 and Q_0 are the operating points of the loads and V_0 is the bus minimum voltage. By setting the exponents to 0 and 1 the load would represent a constant power PQ and a constant current load respectively.

Also, as shown in Figure 3.9, the network includes two 300 and 450 KVar shunt capacitance as reactive power compensation respectively at buses 844 and 848. These two capacitor banks are preserved in all three test cases with or without DGs. The UG transformer is a 2.5 MVA 69/24.9 kV step down and the other one is a 500 KVA 24.9/4.16 kV.

The IEEE test case does not include the over current protection scheme which has been discussed in the following section. The result which has been obtained from the

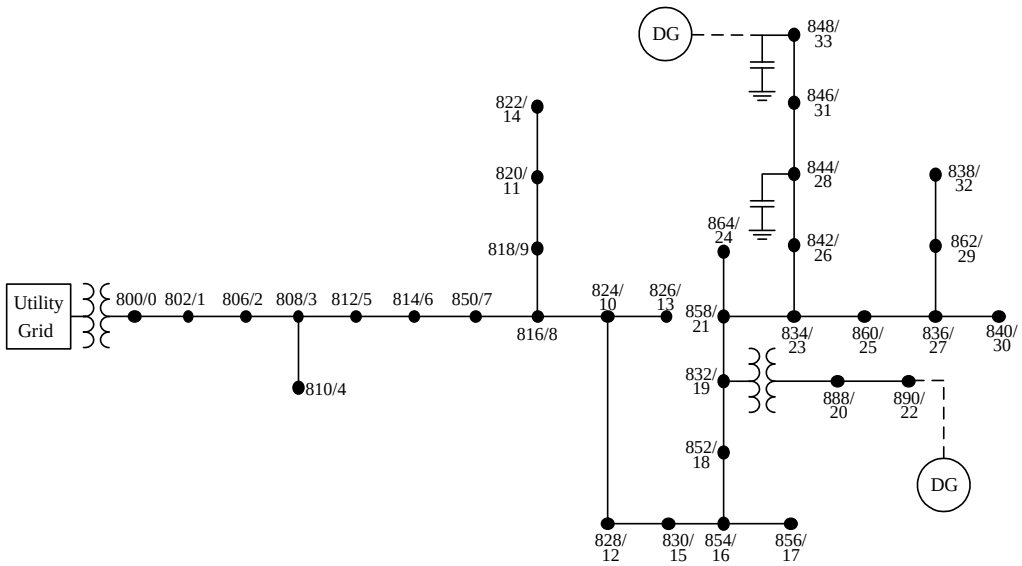

Figure 3.9 IEEE 34-Bus Distribution Network Test Feeder

simulated case shows a good agreement in the case of voltage profile, power flow, and total active and reactive power consumption with respect to the ignored OLTCs. Three scenarios have been considered to investigate the current section. The first case is the IEEE simulated base case while two other cases are networks incorporating two DGs with high penetration in their branches. The second scenario uses two 1 MVA synchronous generators with 0.82 P.F and the third scenario contains two 480V DFIG wind turbines with 1 MVA capacity. DGs buses have been chosen based on the discussions presented in [10] and all DGs are connected to the network using a step-up transformer beside their own interconnection.

Considering the critical case for evaluating DGs' effects on protection systems, just two DG types are designated with the highest penetration and the two most controversial interconnections. Synchronous generator fault current and contribution depends on pre-fault voltage, sub-transient and transient of the machine, while it generally has a good contribution through fault current up to 500-1000% of nominal current at least for first few cycles [10, 11]. DGs interconnection fault play a significant role in their fault condition responses whether or not DG has a rotary torque and electromagnetic field is the first provision. Inverter manufacturers protect their power converters by setting maximum currents and specific time for transient and fault conditions. The current limits can vary within 1.2 to 2.0 per unit of nominal current [11].

Spreading the generators throughout a radial network and attempting to produce the power on consumption sites decreases the transmission power loss. Hence, as it has been discussed in section 3.2.2 and can be deduced from the Figure 3.10 voltage profile does not obey the conventional reducing manner in base cases (without any DG integrated). It is clear from Figure 3.10 that the voltage profile is drastically increased by adding Synchronous DGs, especially in buses far from utility grid. DFIG DGs also exhibit the same results. Another important point here is the excessive voltage profile in some buses after integrating synchronous DGs. As mentioned above, synchronous DGs have been regulated in this simulation to cooperate in reactive power production, hence their impacts in voltage profiles are more significant. However, this demonstrates the concern that an excessive voltage profile may happen, particularly in buses with lightly loaded DGs after integration.

After approving results yielded in the voltage profile section (3.2.2) in the above plot, we can also re-check the trend accuracy of results which have been presented in the fault current level section (3.2.3). Therefore various fault scenarios have been tested to compare the different fault current levels in three different cases with different DGs. Table 3.4 presents a summary of the fault current levels yielded by 3-ph, LLG, bolted LG, and high impedance LG. One can deduce that adding synchronous DGs roughly doubles the 3-phase fault currents, while DFIG increases it drastically. As the fault current reduces by going down the table the DGs' effect decreases. For instance Sync DGs increased single line to ground fault (with 200 ohms fault resistance) current by 0.47 p.u at bus 18 and by 0.39 with the DFIG integration case.

Although all types of DGs improve the voltage profile and, as generally stated before, increase the fault in current level is hard to be stated as general as the voltage profile. A precise categorization is needed to reach the point of formulating the effect of all DGs on the protection system and to be able to build an adaptive protection scheme to provide secure feeders with active branches. Some DGs, such as synchronous generators or micro turbines, usually do not use power electronic base power converters to synchronize with the network. This is why DGs depend on the impedance they see during the fault may contribute to the fault current even ten times

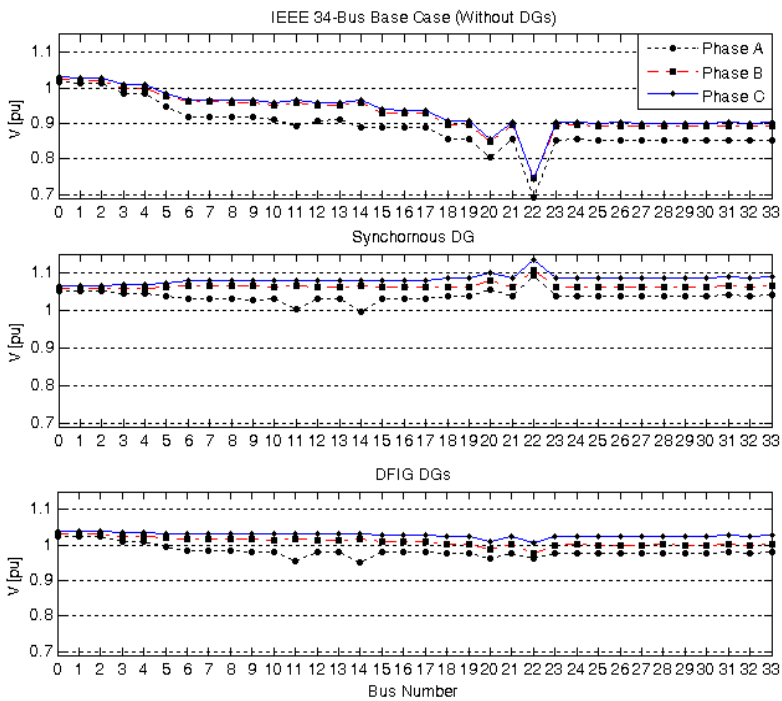

Figure 3.10 Voltage Profile for: a) Base Case b) Sync DG c) DFIG

Table 3.4 Fault Current Level

Fault Type	Bus	Base Case (no DG)	Sync DG	DFIG DG
3-Phase	10	9.19	13.74	11.46
	26	6.37	10.96	8.07
	30	6.18	10.52	7.88
LLG	9	9.22	13.08	11.07
	18	5.86	10.30	8.20
	25	5.39	9.70	7.69
LG(B)	9	7.78	9.81	8.99
	18	4.81	6.92	6.12
	25	4.49	6.48	5.71
LG(Z)	9	1.7	1.97	1.86
	18	1.43	1.84	1.71
	25	1.41	1.81	1.66

more than their nominal current. While the other DG types such as DFIG, PV, FC and so on have to use a converter to connect to the power networks. This DGs interconnection, which mostly consists of a back-to-back power converter, regulates the DG output voltage, frequency, and power. Manufacturers put limits on these interconnection packages to switch off in case of current exceeds nominal. This current can vary from 1.2 to 2.0 per unit while those inverters can feed a fault current transient at most 4 times their nominal current for less than a cycle. DFIG DG has been used in a current study and has the maximum current limit of 40 % more than its nominal current.

Figure 3.11 illustrates the 0.5 per unit decrease in UG fault current contribution. The green curve is related to the case with DFIG DGs integrated and the red curve depicts the most decrease in the current share presents the case with synchronous DGs

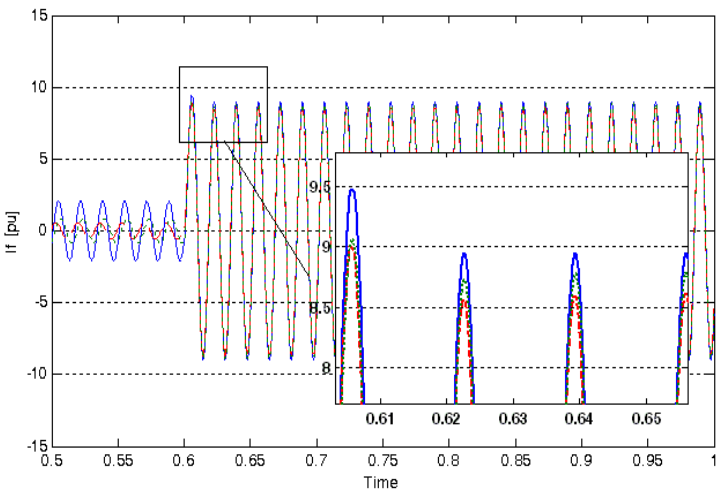

Figure 3.11 Utility Grid Contribution in Fault at Bus 32

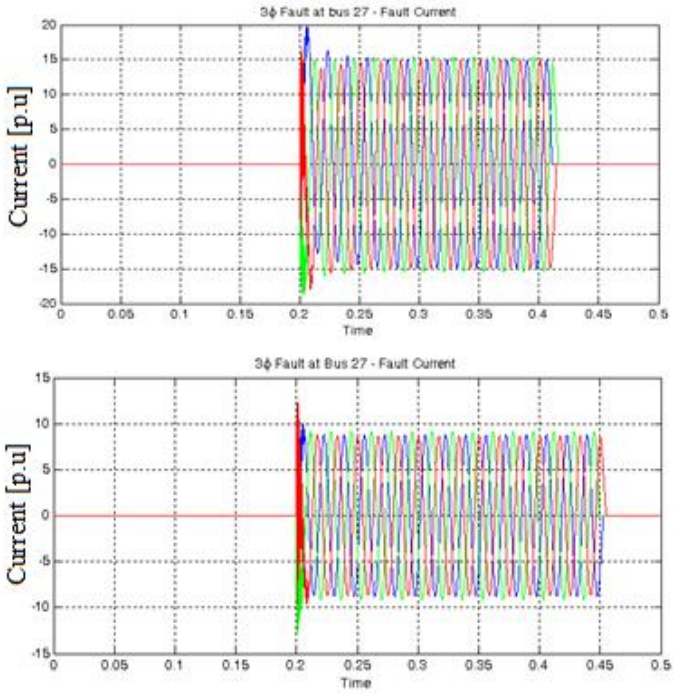

Figure 3.12 Utility Grid Contribution after DG Integration

integrated in network. One can understand that by decreasing the fault current share injecting from the utility grid during fault, all the relays sensing on the UG principal branch should be reconfigured. Almost always, the UG branch is the main and longest feeder with a big number of relays installed on it. This change obliged us to regulate all the relay settings to be compatible with the new power system situation which can be done remotely using CPU.

Figure 3.11 and 3.12 present the responses for a bolted 3 phase to ground fault happening at bus 27. The fault current increase is significant in the plots. Figure 3.11 depicts the system response without any integrated DGs. This is that the fault current is roughly 8 per unit which is almost half of the fault current magnitude in the case with integrated DGs which has been shown in 3.12. It should be mentioned that these fault scenarios have been tripped and cleared by the relay's command. This is the reason that the case with no DG has been cleared after t=0.45 and the case with integrated DGs cleared on 0.412 second.

As mentioned before, test cases in this study did not originally include an over current protection system. This is why a robust coordinated protection system using OCR 51 has been designed for them using the simulated relay. The relay design procedure and its details have been covered in section 2.3.1. The critical challenge in

the OCR protection system design is to maintain the relay's coordination and system's selectivity. Figure 3.13 shows that 12 normal inversed (IDMT) OCR have been employed to sketch the protection scheme. Using OCR 51 without dividing the network into protective zones lead us toward the same problem mentioned in using DT OCRs, that is, high trip time in upstream feeders. The protection system policy in 4 designated zones is that each zone has its own primary and backup protection. Hence the zones are not responsible to support each other while their inter-area backup policy should maintain the minimum Coordination Time Interval (CTI=0.2 s). CTI is the least time gap between OCRs Time Current Characteristics (TTC) curves which ensures that the backup relay doesn't trigger because of circuit breaker, switches, CTs, or other mechanical part delays or malfunctions. Because of the unbalanced nature of the case the OCR protection system design has been done separately for all three phases.

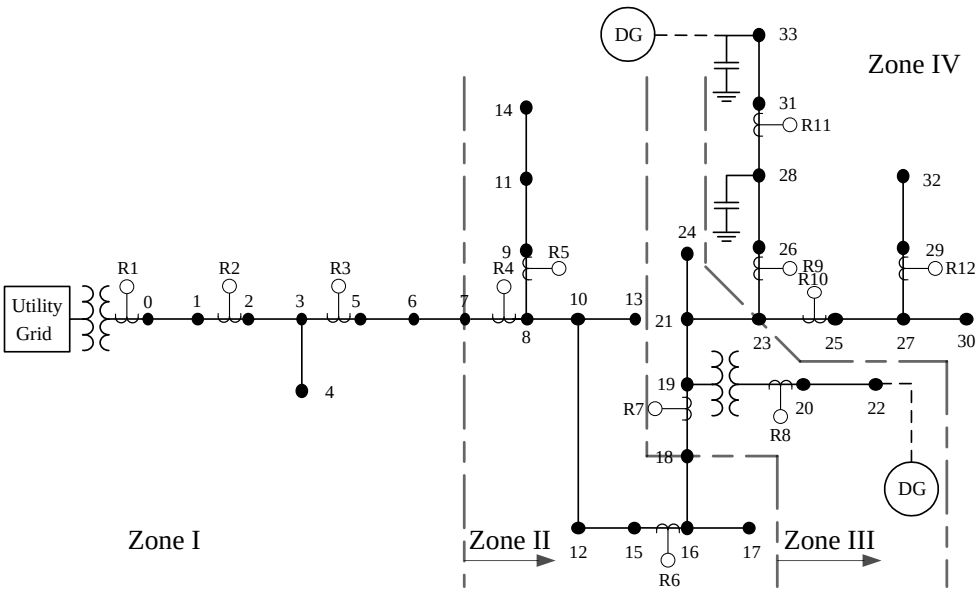

Figure 3.13 Over Current Relays Allocations Inside Protective Zones

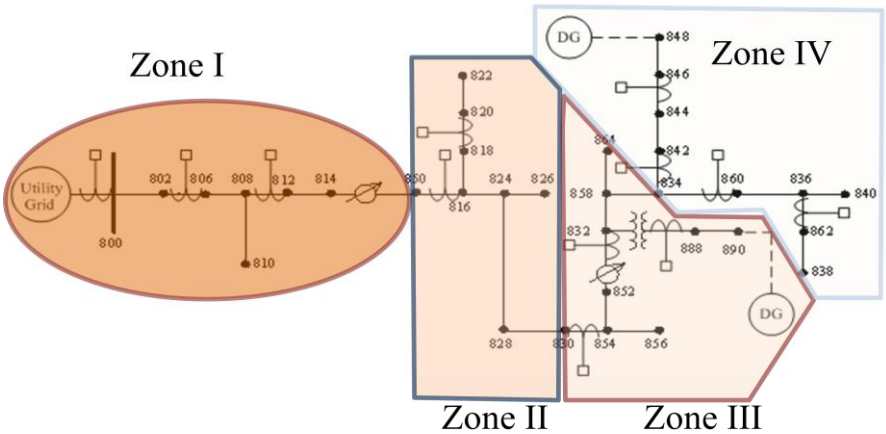

Figure 3.14 OCR Protection System and Its Detailed Zones and Buses

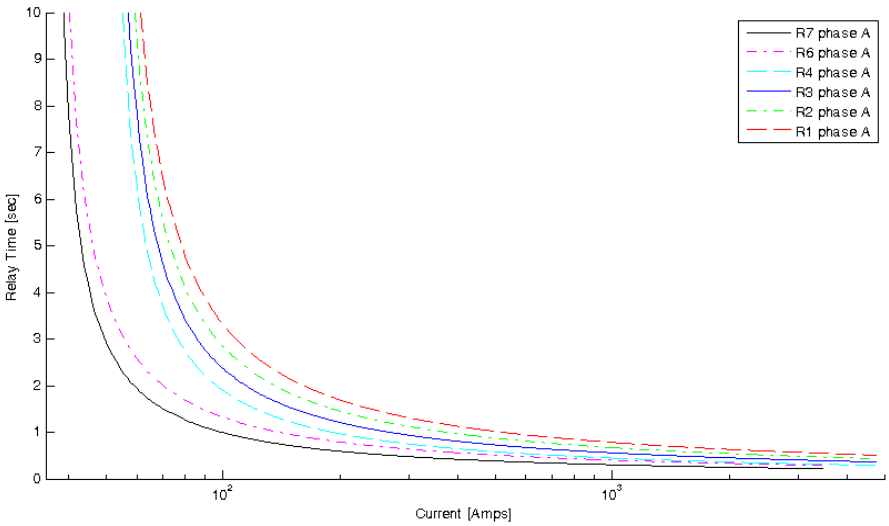

Figure 3.15 OCR Coordination Curves for Zones I to II

3.3.2 Feeders Nominal Current

The IEEE 34-bus dominant feature consists of a vast variety of electrical elements such as real distribution feeders. This feature eases the way towards the discovery of more inconspicuous impacts of DGs integration where one may find more in a practical study. Distribution feeder equipment such over current relays, circuit breakers, surge arresters, and bus sectionizers have been designed to work under a nominal current. While these mediums can also tolerate a certain amount of picks and disturbances within their defined electrical, thermal, and mechanical limits. In a competitive market atmosphere these limits have been tightening to actual work conditions for more profit.

As mentioned before, an IEEE 34-bus includes loads which are considered constant impedance loads (Z). These loads, representing a constant Z, consume active and reactive power based on their terminal's voltage. This means a change in bus nodes can make a

noticeable difference in the power consumption of these loads. As a matter of fact, DGs installation improves the bus's voltage profile, which leads to an increase on constant Z loads, nominal currents, and subsequently results in a greater increase in fault transient picks or inrush currents. This impact can disable the circuit breakers and switches to terminate the current. This can also affect the wiring and transmission line efficiency since they all have been designed for the previous current level. For example, in this study a lateral feeder with bus number 24 which has a constant Z load has had a nominal current equal to 0.24 p.u. before DGs' integration. However, after DGs employment this normal current increased by 8% which is noticeable. This phenomenon can be negligible in feeders with less constant Z loads. Considering feeders consist of large number of such loads, it will definitely interfere with the protection scheme's normal work condition and with other equipment. This means a tightly designed and coordinated overcurrent protection can consider an overload or inrush current as a fault current and consequently command a false trip to the related circuit breaker. On the other hand, it can be possible that circuit breakers and switches fail to work properly or may result in producing a large amount of surges which lead to the incapability in arc extinguishing.

3.3.3 OCR Miscoordination

The art of designing a robust and coherent protection system is directly referred to as relays logic and coordination. Dividing a network into separate protective zones and managing inside zone policy and also zone interactions are the factors which play a significant role in the protection system's effective response. Hence, miscoordination is the most famous and dangerous side effect of DGs integration with currently working networks. It is useful to mention that all the time information presented bellow provided by fault time reference.

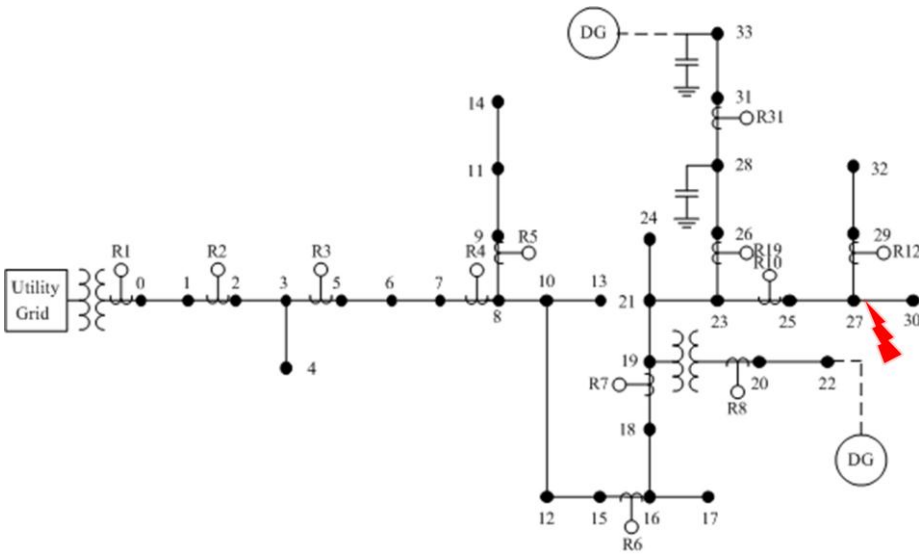

Figure 3.16 OCR Miscoordination for Fault at Bus 27

Many simulations have been done resulting in relay miscoordination as a result of DGs integration. Table 3.5 shows the results for a 3phase bolted fault occurring at bus 27. As shown in the table in base case OCR 51, relay 10 correctly diagnosed the fault condition and responded to it by determining a 0.25 second trip time after the fault happening time. Also, relay 7 supports the primary protection by considering a 0.88 second period to trip after fault time. Considering the fact that these relays are located in different zones, the coordination time gap between them which is 0.63 second, is a proper secondary support tolerance time. However, in synchronous DGs case you can see that OCR 10 trip time is significantly decreased as a result of the change in fault current level. On the other hand, although relay 9 and 7 show an appropriate time for backup protection, relay 11 trips with almost every primary relay. This is a result of the change in fault current share and direction in different branches since relay 11 is not supposed to sense a generator fault current in its feeder. The same condition is resulting from DFIG in cases with less magnitude in time deviations in comparison with Sync cases.

Table 3.6 also illustrates another significant case lead into major incoordination among protection relays. A line to line to ground fault happened at bus 18 which led to a 0.77 second trip time and R4 backup with a 0.92 second trip time in the base case. One can see that Sync cases R6 and R7 perfectly play the primary protection rule while the backup protection relays interfere with their task. One can see that relays 8 and 9 tripped sooner than the primary protection relays.

Table 3.5 OCR Miscoordination for Fault at Bus 27

Fault	Base Case		Sync DG		DFIG DG	
	Primary	Backup	Primary	Backup	Primary	Backup
B27 3Ph	R10: 0.25	R7:0.88	R10: 0.19	R9:0.42 R7:0.6 **R11: 0.25**	R10: 0.22	R9:0.53 R7:0.61 **R11: 0.38**

Table 3.6 OCR Miscoordination for Fault at Bus 18

Fault	Base Case		Sync DG		DFIG DG	
	Primary	Backup	Primary	Backup	Primary	Backup
B18 LLG	R6:0.77	R4:0.92	R6:0.78 R7:0.63	R4:0.9 **R8:0.56 R9:0.43**	R6:0.69 R7:0.81	R4:0.94 **R8:0.83 R9:0.52**

3.3.4 OCR Blinding

The first step for a protection system to ensure system security is the capability of fault recognition. Overcurrent protection systems do this by comparing the measured current with a set pick up current. This is a straightforward approach, particularly when the normal current and fault current would have a constant, and also when they always have the same direction in radial networks. While this case, which stands for base case without any DG, does not hold for DG integrated cases. Consequently, adding DGs can change the current path in both normal and faulty conditions. This incident results in a protection scheme unable to detect a fault, particularly protection blindness or faults happening with connecting impedance. Also this integration changes the current phase in different buses which can be investigated using Phasor Measurement Units (PMU) in separate study.

Table 3.7 Overcurrent Protection Response

Fault	Base Case		Sync DG		DFIG DG	
	Primary	Backup	Primary	Backup	Primary	Backup
B28 LLZ	R9:1.02	R7:1.68	R9:5.78 R11:0.31	**None**	R9:7.31 R11:043	**None**

Relays measured current and calculations demonstrates that after Sync DGs' integration, active power is provided by utility grid up to bus 16. This is a change in current and power paths in all downstream feeders under bus 16. The same results are carried out for active power using DFIG DGs, since they are the same, in active power production. Table 3.7 illustrates the protection system response to a LLZ fault which happened at bus 28 with 200 ohms fault impedance. It can be deduced from the table, primary overcurrent relay in which R9 correctly detects the fault current and considered a 0.73 second trip time after the fault happened. Backup relay R7 is in the back zone which has TT=1.38 seconds to support R9 with a good time coordination regarding the fact that they are located in separate zone. However, in sync DG cases, as a result of large amount of current injected by DG2, R9 does not see as much current as it has been measuring in the base case. Therefore, relay 9 shows a 3.78 second time interval after the fault happened, which is a desperately long time for such a fault with almost 5 fault current per unit. On the other hand, besides R11 which plays a primary

Table 3.8 Overcurrent Protection Response

Fault	Base Case		Sync DG		DFIG DG	
	Primary	Backup	Primary	Backup	Primary	Backup
B20 LLZ	R8:12.1	R7:36.6	**None**	**None**	**None**	**None**

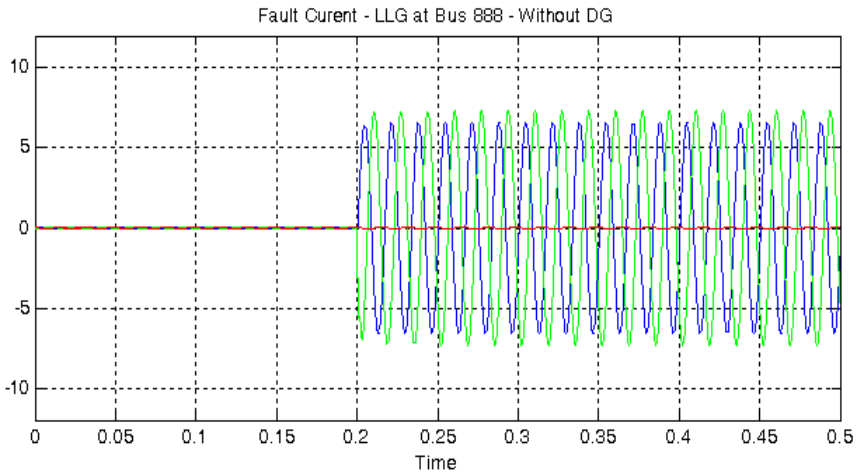

Figure 3.17 Fault Current for Fault at Bus

relay because of DG2 injected current, none of the other relays detected the fault current to back up the R9 operation.

Protection system blindness because of DG integration is more likely due to the highly loaded distribution networks with a long feeder connecting them to the upstream substation. This means the utility grid is facing large impedance reaching the fault point leads to less contribution after DGs integration. On the other hand, such a network demands numerous DG units to enhance the voltage profile and provide power, which directs to more current path cross sections, detours for fault current which disables the former protection system to detect the fault condition.

Chapter Four

Phasor Measurement Unit (PMU) And K-means clustering

4.1 Overview

A synchronized measurement device is quite necessary for smart power system protection. Most researchers uniformly agree about applying the Phasor Measurement Unit (PMU) to estimate the system state and accurately measure the buses' signals. This section investigates different algorithms to estimate phasor information by Phasor Measurement Units (PMU). Power Systems are getting more complicated and subsequently their supervision, control, and protection are more critical. Various systems such as Wide-Area Measurement Systems (WAMS) or Central Protection Unit (CPU) should be employed for this goal. All of these supervisory systems rely on PMU technology synchronized by a Global Positioning System (GPS). Therefore, PMU accuracy and performance during different power system working conditions has a severe impact on the system state estimation. The PMUs ability in accurately tracking desired phasor data is an important feature, particularly during disturbances. This has a critical impact on the supervisory system in maintaining system reliability and security as well as performing precautionary measures by CPU to prevent aggravating scenarios. It has been rigorously shown that Discrete Fourier based algorithms are the best methods in the digital world to implement in PMU devices for extracting phasor. Off-nominal frequency and performance during different working conditions have been studied in this section. Although other PMU algorithms have been explained in the summary, robust simulation has been performed in MATLAB

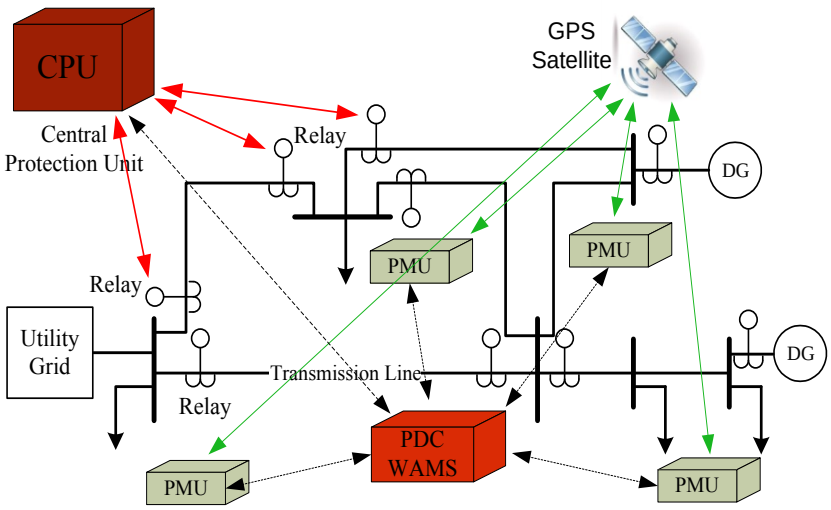

Figure 4.1 Central Protection Unit and PMU Importance

Simulink to compare DFT and SDFT as two of the main algorithms which have been considered for this study. On the other hand, methods have been discussed in this section to analyze the very large amount of PMU data. K-means clustering, specifically, is provided along with an initialization algorithm. The proposed algorithm, which has been explained, increases the K-means' efficiency and accuracy and improves its redundant results with less computational burden. The importance of this proposed algorithm has been thoroughly discussed along with comparisons of the actual simulated PMU data in a simplified power system.

4.2 PMU Algorithms

One of the major concerns in current large interconnected power systems is maintaining system stability and security. This goal is more critical when power systems are working close to their boundary limits or are expected to work in a sophisticated situation with various DGs integrated in the system. On the other hand, terms such as smart grid are aimed at integrating decisive DGs into the network with adaptive protection, diagnosis, and prevent aggravating disturbances to avoid outrageous blackouts while also reaching goals such as smart and intelligent islanding. Supervisory and state estimation structures such WAMS and CPU has been innovated to make the real smart grid more feasible in power systems. However, all state of the art innovations in grid supervision and secure control rely on PMUs technology for its information.

PMUs and digital relays are currently the back bones of power system supervision and protection methods. A device which measures the voltage and current signals' phasors in a particular bus with a consistent stream of synchronized data is called a Phasor Measurement Unit (PMU). IEEE Std. C37.118 and IEC 61850 determine the Relays' and PMUs' required accuracy and standards [12-15]. PMUs' accuracy plays a critical role in any state estimation or supervisory algorithm. This means PMUs' errors, which clearly increase during faults or disturbances, may misdirect systems such as CPU and influence its stated performance.

Many algorithms have been developed for PMU calculations. Martin Morf and Thomas Kailath developed the Least-Square Root method in their article in 1975 [13]. Large amounts of numerical calculations and matrix manipulations, needed for matrix inverse calculations and possibility for singular matrix, are the method's drawbacks.

On the other hand, this method has issues because of huge numerical calculation burden as it is been explained in Lang and Laakso's article in 1994 [14]. Lobos and Rezmer showed in their paper that the Prony method is significantly better than the DFT method, especially when using more than 20-length array [15]. However, it is also mentioned that prony demands complicated pre-filtering and window function to reach such a performance since it is very vulnerable to signal noises [16]. However, methods using signal's Fourier series such as the Discrete Fourier Transform (DFT) and the Smart DFT are more well-known and popular. Although these methods also need suitable filtering, but using signals Fourier coefficients and their simplicity enabled them to be used for current digital devices with minimal computational burden. Hence this section focuses on DFT and SDFT comparison to investigate their performances in extracting signal phasor data, particularly for signals which are representing actual power signals during fault and disturbances such as change in frequency, phase, and other off-nominal working conditions.

4.3 Mathematical Principles of DFT and SDFT

This section presents the algorithm of DFT and SDFT that estimates a signal phasor data [16, 17]. The measured electrical signal for purposes of phasor calculations can be considered as a sinusoidal (probably corrupted by additional harmonics, noises, additional filtering gain and delays) of frequency $\omega_0=2\pi f$ as follows:

$$x(t) = X \cos\big(\emptyset(t)\big) = X\cos(\omega_0 t + \varphi) \tag{4.1}$$

$$\omega_0=2\pi f \tag{4.2}$$

Where X: Signal amplitude of the Voltage/Current signal

f : is the signal frequency (60 Hz)

φ: the phase angle of the Voltage/Current signal

The signal x(t) can be conventionally represented as its phasor or complex form as:

$$\bar{x} = X\, e^{j\varphi} = X\cos\varphi + jX\ \sin\varphi \tag{4.3}$$

Therefore x(t) can be expressed as:

$$x(t) = \frac{\bar{x}e^{j\omega t}+\bar{x}^{*}e^{-j\omega t}}{2} \tag{4.4}$$

Where * denotes the complex conjugation. Sampling is quite necessary for Discrete Fourier Transform execution and it is also inevitable for the real PMUs application in digital systems using ADCs. As mentioned in a variety of literature, sampling frequency does not affect the result accuracy as long as it meets the Nyquistrate [17]. Hence N, which is the number of samples per cycle, can vary significantly. Sampled signal in equation. 4.1 can be shown as follows:

$$x(k) = X \cos(\omega \frac{k}{60\,N} + \varphi) \tag{4.5}$$

By calculating the x(t) signal DFT series, the fundamental frequency component will be:

$$\hat{x}_r = \frac{\bar{x}}{N} \sum_{k=0}^{N-1} x(k+r) e^{-j\frac{2\pi k}{N}} \tag{4.6}$$

Using equations 4.3 and 4.4 and considering fundamental frequency deviation:

$$\hat{x}_r = \frac{\bar{x}}{N} \sum_{k=0}^{N-1} e^{j2\pi(60+\Delta f)\frac{k+1}{60N}}. e^{-j\frac{2\pi k}{N}} + \frac{\bar{x}^*}{N} \sum_{k=0}^{N-1} e^{-j2\pi(60+\Delta f)\frac{k+1}{60N}}. e^{-j\frac{2\pi k}{N}} \tag{4.7}$$

Rearranging the equation results in:

$$\hat{x}_r = \frac{\bar{x}}{N} e^{j\frac{2\pi}{N}(1+\frac{\Delta f}{60})r} \sum_{k=0}^{N-1} e^{j2\pi\frac{\Delta f}{60N}k} + \frac{\bar{x}^*}{N} e^{-j\frac{2\pi}{N}(1+\frac{\Delta f}{60})r} \sum_{k=0}^{N-1} e^{-j2\pi\frac{(2+\frac{\Delta f}{60}}{N}k} \tag{4.8}$$

Using the following identity:

$$\sum_{i=0}^{N-1} (e^{j\theta})^i = \frac{\sin\frac{N\theta}{2}}{\sin\frac{\theta}{2}} e^{j(N-1)\frac{\theta}{2}} \tag{4.9}$$

Equation 4.8 can be expressed as 4.10,

$$\hat{x}_r = \frac{\bar{x}}{N} e^{j\frac{2\pi}{N}(1+\frac{\Delta f}{60})r} \frac{\sin\frac{N\theta_1}{2}}{\sin\frac{\theta_1}{2}} e^{j(N-1)\frac{\theta_1}{2}} + \frac{\bar{x}^*}{N} e^{-j\frac{2\pi}{N}(1+\frac{\Delta f}{60})r} \frac{\sin\frac{N\theta_2}{2}}{\sin\frac{\theta_2}{2}} e^{j(N-1)\frac{\theta_2}{2}} \tag{4.10}$$

Where $\theta_1 = \frac{2\pi\Delta f}{60N}$ and $\theta_2 = -\frac{2\pi(2+\frac{\Delta f}{60})}{N}$.

By rearranging equation 4.10 we reach to the objective equation:

$$\hat{x}_r = \frac{\bar{x}}{N} \frac{\sin\frac{N\theta_1}{2}}{\sin\frac{\theta_1}{2}} e^{j\frac{\pi}{60N}(\Delta f(2r+N-1)+120r)} + \frac{\bar{x}^*}{N} \frac{\sin\frac{N\theta_2}{2}}{\sin\frac{\theta_2}{2}} e^{-j\frac{\pi}{60N}(\Delta f(2r+N-1)+120(r+N-1))} \tag{4.11}$$

Therefore we can define A_r and B_r as:

$$A_r = \frac{\bar{x}}{N} \frac{\sin\frac{N\theta_1}{2}}{\sin\frac{\theta_1}{2}} e^{j\frac{\pi}{60N}(\Delta f(2r+N-1)+120r)} \tag{4.12}$$

$$B_r = \frac{\bar{x}^*}{N}\frac{\sin\frac{N\theta_2}{2}}{\sin\frac{\theta_2}{2}} e^{-j\frac{\pi}{60N}(\Delta f(2r+N-1)+120(r+N-1))} \tag{4.13}$$

Therefore the equation 4.11 can be written as:

$$x_r = A_r + B_r \tag{4.14}$$

DFT and SDFT algorithms are completely the same until this point. Actually this similarity, which originates from Fourier application, enables both of them to take advantage of recursive computations [18]. Conventional DFT method assumes that the second term of frequency deviation in eq. 4.14 (B_r) is small enough to be omitted. Hence, using $A_r$results in calculating the signal amplitude, phase, and frequency. In the simulated block used for following presented discussions, the calculated phase derivative has been used to correct the frequency deviation errors based on the equation:

$$f = f_0 + \Delta f = f_0 + \frac{1}{2\pi}\frac{d\varphi}{dt} \tag{4.15}$$

However in SDFT algorithm both terms A_r and B_r will be considered to reach a precise phase and especially frequency estimation during deviations. The exact solution for SDFT demands parameter a definition which is expressed below:

$$a = e^{j(-\frac{\pi}{60N}(2\Delta f+120))} \tag{4.16}$$

By multiplying eq. 4.14 with ‘a’ and considering eq. 4.11 we reach to following relations:

$$A_{r+1} = A_r \times a \tag{4.17}$$

$$B_{r+1} = B_r \times a^{-1} \tag{4.18}$$

Then:

$$\hat{x}_{r+1} = A_{r+1} + B_{r+1} = A_r \times a + B_r \times a^{-1} \tag{4.19}$$

$$\hat{x}_{r+2} = A_{r+2} + B_{r+2} = A_{r+1} \times a + B_{r+1} \quad \times a^{-1} \tag{4.20}$$

If we multiply ‘a’ to the both sides:

$$\hat{x}_{r+1} \times a = A_r \times a + B_r \tag{4.19}$$

$$\hat{x}_{r+2} \times a = A_{r+1} \times a + B_{r+1} \tag{4.20}$$

Subtracting 4.14 from 4.19 and 4.19 from 4.20 results in:

$$\hat{x}_{r+1} \times a - \hat{x}_r = A_r(a^2 - 1) \tag{4.21}$$

$$\hat{x}_{r+2} \times a - \hat{x}_{r+1} = A_{r+1}(a^2 - 1) \tag{4.22}$$

Dividing the two equations:

$$\frac{\hat{x}_{r+2} \times a - \hat{x}_{r+1}}{\hat{x}_{r+1} \times a - \hat{x}_r} = \frac{A_{r+1}}{A_r} = a \tag{4.23}$$

Rearranging the eq. 4.23 results in the key quadratic formula which results in calculating 'a' as follows:

$$a = \frac{(\hat{x}_r + \hat{x}_{r+2}) \pm \sqrt{(\hat{x}_r + \hat{x}_{r+2})^2 - 4\hat{x}_{r+1}{}^2}}{2\hat{x}_{r+1}} \tag{4.24}$$

$$f = 60 + \Delta f = \cos^{-1}(Re(a)) \times \frac{60N}{2\pi} \tag{4.25}$$

Therefore by using SDFT algorithm taking both frequency deviations terms we can extract the signal phasor information as shown below:

$$A_r = \frac{\hat{x}_{r+1} \times a - \hat{x}_r}{a^2 - 1} \tag{4.26}$$

$$X = |A_r| \times \frac{N \times \sin(\frac{\pi \Delta f}{60N})}{\sin(\frac{\pi \Delta f}{60})} \tag{4.27}$$

$$\varphi = angle(A_r) - \frac{\pi}{60N} \times (\Delta f \times (N - 1)) \tag{4.28}$$

It should be mentioned that eq. 4.1 in the first step of presenting the DFT and SDFT just contains the signal fundamental first harmonic. However, by assuming the rest of the harmonics in the first step, the higher order SDFT can be derived, which results in more accuracy and robustness in estimating signal frequency during disturbances and off-nominal frequency working conditions. Although this advantage is just related to SDFT and DFT is the just explained simple algorithm, even SDFT have some limits in employing signals harmonics [18]. Using signal higher order harmonics accompanies computational burdens and delays. Delay, computational burden, and deployed microprocessor ability to process the calculation play a significant role in convincing the vendors not to use signal higher order harmonic but implement digital filters.

4.4 DFT and SDFT Comparison

Simulation results and plots are shown in this section along with the comparative discussion. Both DFT and SDFT algorithms have been narrowly modeled in MATLAB Simulink to enable us to test various signal conditions and investigate both approaches. As mentioned, the number of samples does not have any significant impact on the PMUs' output accuracy or other response characteristics. If the sampling frequency would be $F_s = Nf$, it means that we have N samples per cycle and sampling period is$T = {}^{1}/_{F_s}$. The sampling frequency and number of samples per cycle determine the window length [19]. As it mentioned in the previous sections, pre-filtering is a quite necessary step in processing the signal against noises and other issues such as frequency deviation or DC off set. The signal waveform will be filtered by a smoothening window which can play an important role on the PMU's output. Many researches have been discussing various complicated smoothing windows, in particular Hamming, Blackman, Taylor, and rectangular window. However, in this study we are using the rectangular window to have a fair comparison with minimum filtering compensation and collaboration in the PMU's output generation [19]. However, it is clear that using a rectangular window comes with some disadvantages particularly for fundamental frequency deviated signals that result in fair assessment and comparison for the worst cases. Various scenarios with different signals have been considered to investigate the simulated blocks with a focus on frequency deviation as a vulnerable point for Fourier based PMUs. Constant off-nominal frequency working condition, step change in signal frequency, and ramp change in frequency are the scenarios which have been studied. The PMUs' frequency estimation output and also

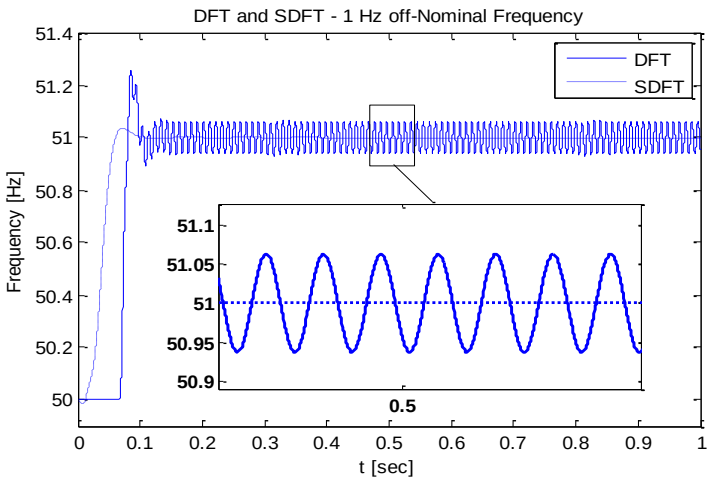

Figure 4.2 DFT and SDFT in off-Nominal Frequency (51Hz)

impacts on signal amplitude calculation have been covered.

Fourier based algorithms performance for estimating signals' waveform amplitude, phase, and frequency are controversial for off nominal frequency. Although frequency has many definitions, most of literatures are unified in calculating the frequency based on the signal angular phase speed [20]. Figure 4.2 illustrates the DFT and SDFT performance in measuring the signal frequency. Signal real frequency is 51 Hz while, as mentioned in section II, both DFT and SDFT have been expanded based on the 50 Hz fundamental signal. Hence we are expecting some errors in the PMUs' output. Taking formula 4.14 into account, DFT has a significant error comparing to SDFT as of ignoring the second term which partially observes the off-frequency deviation. Therefore the DFT result oscillates around the actual frequency value (51 Hz) with 0.65 amplitude which results in 1.3%Total Vector Error (TVE). Although this error is relatively significant because, the simulated PMU is estimating a signal with a different fundamental frequency than what PMU is designed for. According to equation 4.15, SDFT considers the off-nominal frequency and measures it by including equation 4.14's second term. That is why SDFT is able to accurately estimate the exact frequency of the waveform with constant off-nominal frequency. As illustrated in Figure 4.2, SDFT conducts a zero error in estimating the waveform frequency with constant frequency deviation, regardless of the deviation magnitude.

Figure 4.3 depicts the DFT results in calculating the waveform amplitude. It should be mentioned that a signal amplitude of 100 has been chosen in this study hence the

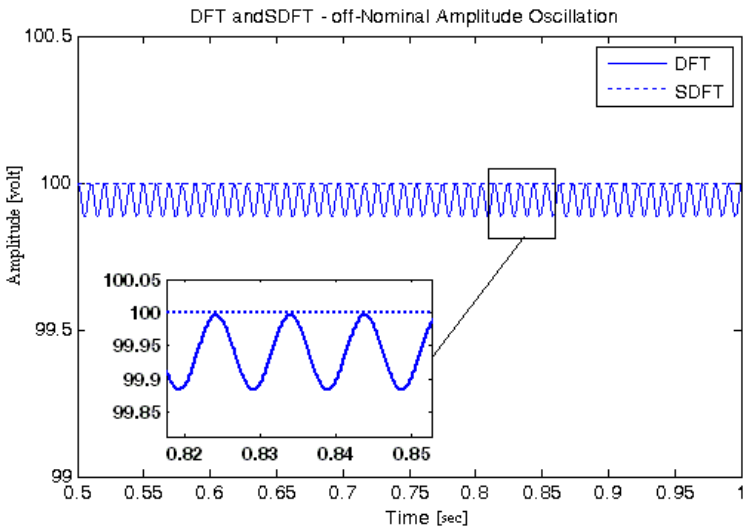

Figure 4.3 DFT Amplitude Oscillation

estimation error is equal to the TVE and there is no need for the simple TVE calculation. As a result of the signal 51 Hz frequency, the Fourier series should not be truncated after the fundamental coefficients. This is not consistent with DFT algorithms, but it is consistent with SDFT. Therefore, as plotted in Figure 4.3, DFT experiences 0.1% error in calculating the waveform amplitude for 1 Hz deviation. Since power systems rarely experience more than 10 Hz transient frequency deviation, the DFT performance is acceptable, while SDFT is surely more preferable due to its compatibility with IEEE C37.118 estimation error standards. A step change in the signal frequency is also investigated for analyzing and comparing DFT and SDFT performances. In this scenario the signal will maintain a 50 Hz frequency equal to the defined fundamental and experience a step change in t=0.5 second with amount of 5 Hz which is a reasonable and possible case for the power systems application. Figure 4.4 a and b illustrate the DFT and SDFT performances, respectively, in estimating the signal frequency. Both DFT and SDFT show a good performance in tracing the frequency step change, considering the fact that the pre-filtering window is rectangular and also a simple second order filter have been used in the output which may not be optimized in case of response time. However DFT results in spikes with 0.4 Hz error

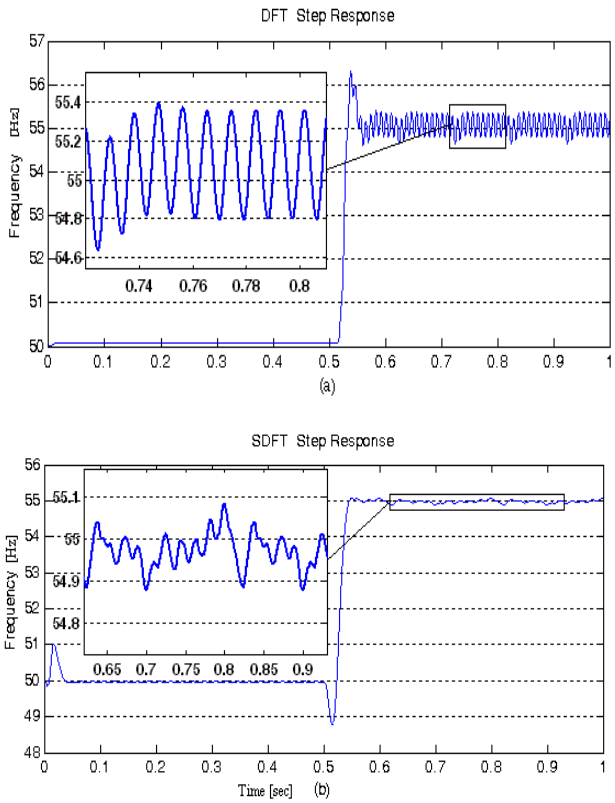

Figure 4.4 5Hz Step change Response: a)DFT b)SDFT

(0.7% TVE) and a steady error equal to 0.3 Hz (0.54% TVE). On the other hand SDFT shows a significantly more accurate estimation to the step change in the waveform's signal. As one can notice in Figure 4.4.b, SDFT has a fast response to the step change and results in a 0.11 Hz frequency estimation error and 0.18 TVE at most. Generally the SDFT scale of frequency estimation error in the case of step response is effectively better than DFT. On the other hand, DFT presents a larger amplitude calculation error as a result of 5 Hz total frequency deviation in comparison with previous case. Since by deviating from the fundamental frequency the Fourier coefficients truncations gets more significant and amount of amplitude calculation error deteriorates in DFT.

Another case which has been investigated for algorithms' performance study is a ramp change in the signal frequency. In this case, the waveform maintains a fundamental frequency (50 Hz) until t=0.5, by which time the signal frequency starts to change. Signal frequency changes as a timely ramp with a slope equal to 4 Hz/second. As can be deduced from Figure 4.5, both algorithms have couples of cycles delay in showing the output which is due to their output filters. However the algorithm

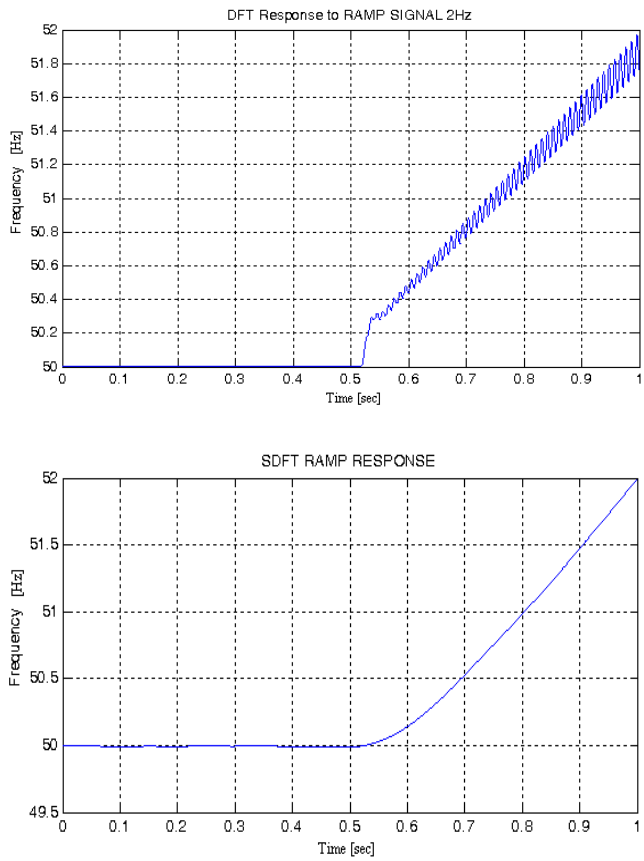

Figure 4.5 2 Hz Ramp Change in frequency a)DFT b)SDFT

compensates this and reaches the actual real frequency. As it mentioned in the previous case, one the most significant issues with DFT which is the aggravating error by deviating more from the fundamental frequency is more obvious here. Figure 4.5.a clearly illustrates the fact that DFT frequency estimation error is expanding by increasing the ramp change. This mean at first the error is ignorable while by raising the frequency harmonics coefficients turn into a significant amount accumulated into the second term.

On the other hand, Figure 4.5.a depicts a good performance from SDFT algorithm with small errors less than 0.05 Hz. However DFT errors aggravate into 0.28 Hz from the signals real frequency. Figure 4.6 depicts the DFT output for the signal amplitude. One can see that the same trend is happening in calculating the waveform amplitude originating from the same reason as explained. It is shown in the Figure 4.6 in the magnified section that as much as the frequency deviates more, the amplitude tends to oscillate more with a lower average. Reducing average of the calculated amplitude also is a result of ignoring Fourier fundamental frequency harmonics.

The present study investigated algorithms for extracting phasor information from the signal waveforms particularly DFT and SDFT. Both of these algorithms are more favorable and preferable comparing to the others proposed for PMU. Various signal scenarios has been used to evaluate algorithms output for different cases. DFT has issues for waveforms with off-nominal frequency deviations. The DFT information error is deteriorating as the frequency deviation increases. However SDFT is showing a better performance in tracking and extracting accurate phasor information from the signals. SDFT yields accurate phasor information mostly regardless of the deviation

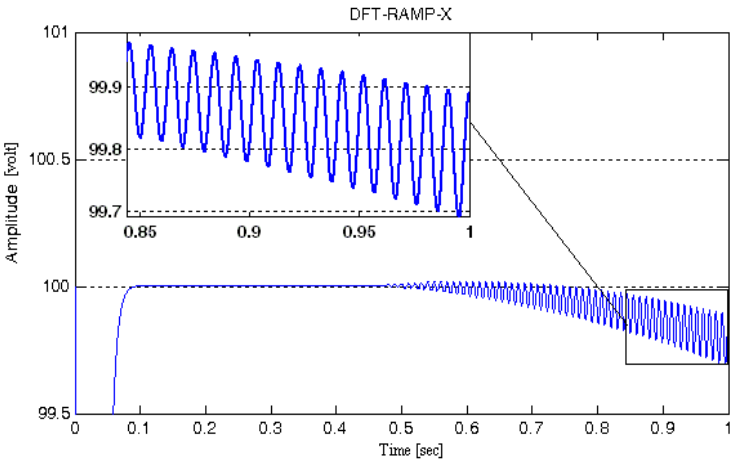

Figure 4.6 DFT Amplitude with Ramp Change in Frequency

magnitude. On the other hand, using DFT algorithm both estimated frequency and amplitude error will aggravate by rise in signal actual frequency from the fundamental. But SDFT maintain a limited amount of error even by change in the processed signal. SDFT also has the capability to use higher harmonics in order to increase the estimation accuracy while large computational burden is an obstacle in expanding the algorithm order.

4.5 K-means Clustering

The K-means clustering is one of the most popular and influential algorithm in data categorization methods. K-means' simple and straightforward formulation made it a widely acceptable method in many fields and applications. This simplicity comes at a price, such as user defined number of clusters, uniformly sized clusters, and different final clusters being sensitive to initial centroids. K-means' sensitivity to initial centroids leads to different clusters per execution with different and relatively large iteration numbers. Different applications have their own initialization and improvement techniques for K-means relying on their particular data traits. Power systems have recently been involved with data mining and clustering due to the fast increase in PMU uses for supervisory, control, and protection goals in smart grids. Large amounts of data streaming by PMU demands simple method with minimum computational burden to meet delay tolerance for various working phases and expectations. This thesis presents an approach to significantly improving K-means clustering algorithm by pre-analyzing the data and finding best initial centroids. Extensive experiments have been made to verify the approach's robustness in reducing the number of iterations and resulting in unique clusters in all executions.

K-means clustering is one of the most popular methods in data clustering. It has been utilized in applications such data mining, knowledge discovery, data compression and vector quantization, pattern recognition and classification, medical imaging, and many other fields involving experimental, statistical, or just large amounts of information[20]. Its simple and straightforward formula with a quite low communicational burden makes it the best option for PMU data manipulation. However, it rarely has been used in electrical power systems' application comparing to its capacity. PMUs' fast data stream demands a simple and adaptive algorithm which is able to adapt to ongoing stream of information. The K-means clustering simplicity and low computational burden comes at a cost. This cost includes user defined number of

clusters, uniformly sized clusters, and being sensitive to initial centroids. Xiong mentioned the fact that K-means clustering tends to produce clusters with relatively uniform sizes even by distinct varied input data. Many studies have covered algorithms to estimate number of clusters [21]. Initial centroids in many applications are more than enough to be determined randomly through the data [21]. However in our data types, K-means' various deviations based on different random initial centroids may play a critical role in the last decision. K-means' final result clusters vary significantly from the randomly chosen centroids within the PMUs data. On the other hand, algorithm number of iterations can be big or very different per each session of execution resulting from a blind start point.

4.6 K-means Clustering Principals

K-means clustering's simple and straight formula is one of the important advantages which made it very popular in many fields and areas. Clustering's problem is the challenge of categorizing a set of data into different groups so that each group's elements hold some similar identities. These identities can be color, weight, position, and even gradient of change, which made the algorithm applicable from satellite and medical image processing to electrical power systems.

Given $\mathrm{X} = \{\mathrm{X}_1, \mathrm{X}_2, \dots, \mathrm{X}_\mathrm{n}\}$as an input set of data which consists of n objects with ddimensions in space of R^d, and the parameter $1 < \mathrm{K} < n$, which is the number of clusters that input needs to be categorized in, K-means clustering should determine Kclusters, including their vectors. K-means does not have a limit on input objects' number of dimensions. That is, each X can be represented as $\mathrm{X}_\mathrm{i} = [\mathrm{x}_{\mathrm{i},1}, \mathrm{x}_{\mathrm{i},2}, \dots, \mathrm{x}_{\mathrm{i,d}}]$, when d can be any positive integer. The clustering algorithm starts by considering K number of points within X to start the algorithm with cluster initial centroids which should be close to their own clusters center of mass by the end of algorithm. One of the disadvantages of K-means is that it is very sensitive to the initial centroids that have been chosen. This dependency relies on the data natural structure [22]-[26]. Therefore choosing random centroids is quite sufficient for some types of data, while it results in completely dissimilar outputs for PMUs types of information, as has shown in section IV. Considering $(\mathrm{M}_1, \dots, \mathrm{M}_\mathrm{k})$centroids for $\mathrm{M}_\mathrm{j}$clusters when $1 \leq \mathrm{j} \leq \mathrm{k}$ and measuring the squared Euclidean distances for X_i enable us to find the nearest centroid to eachX_i.

Therefore the M_j clusters are being constituted with points that are closer to their centroids, comparing their distances to others, that is:

$$X_i \in M_j \leftrightarrow \left\|X_i - M_j\right\|^2 \leq \left\|X_i - M_p\right\|^2 \tag{4.29}$$

For all $1 \leq p \leq k$, $p \neq j$ and with $1 \leq i \leq n$, $1 \leq j \leq k$

$$\left\|X_i - M_j\right\|^2 = d^2(X_i, M_j) = \sum_{h=1}^{d}(x_{i,h} - m_{i,h})^2 \tag{4.30}$$

The formula 4.30 presents the squared Euclidian distance for d dimensional points. Some k-mean algorithms utilize different distant computations which don't have a significant impact on the results in this particular application. However in some fields it may increase the chance to find the global minimum for the final error. As shown above, using 4.30 distant of each X_i will be computed and X_i will be put into cluster (M_j) which its centroid (M_j) is the most closest to X_i. Each cluster contains an error, which is the sum of all its points' distance with its centroid. The goal of K-means is to minimize the clustering error and the overall error will be the sum of all the clusters error which is:

$$E(l) = \sum_{j=1}^{k} \sum_{X \in M_j} \left\|X - M_j\right\|^2 \tag{4.31}$$

Formula above can be presented as bellow, l is the iteration number.

$$E(l) = \sum_{i=1}^{n} \sum_{j=1}^{k} I(X_i, M_j) \left\|X_i - M_j\right\|^2 \tag{4.32}$$

$$I_l(X_i, M_j) = \begin{cases} 1 & X_i \in M_j \\ 0 & X_i \notin M_j \end{cases} \tag{4.33}$$

$E(l)$ is calculated in each iteration. Minimizing this function leads to the best clustering result. Hence either the amount of this function or its change in comparison to previous iterations can be used as the algorithm termination condition. However, the most common termination condition is the fact that no more points will be transferred within the clusters, meaning the K-means algorithm converged to a steady state and satisfied most of the applications. But $E(l)$ termination conditions are more useful for cases with data which may not converge, large amounts of data, or data with significant amounts of noise or uncorrelated points. The condition to terminate the algorithm using the error function can be:

$$E(l) - E(l-1) \leq \varepsilon \tag{4.34}$$

Both centroids and clusters' group of objects will be updated in each of the iterations. Centroids play an important role in K-means number of iterations to converge, ensure the quality of, and stabilize the clustered results in different executions. With the exception of the first loop, in the rest of the iterations, centroids update based on the formula below to approximate the cluster j center of mass used for iteration $\mathrm{l}+1$. Updating the centroids mostly results in a better value for the Error function in the next iteration $(\mathrm{l}+1)$ although divergence is possible, particularly for random initial centroids. Equation 4.35 calculates the mean of the objects which are already categorized in cluster j and $\mathrm{n}_{\mathrm{M_j}}$ is the number of objects in $\mathrm{M}_{\mathrm{j}}^{\mathrm{l}}$.

$$\mathrm{M}_{\mathrm{j}}^{\mathrm{l}+1} = \frac{1}{\mathrm{n}_{\mathrm{M_j}}} \sum_{\mathrm{X} \in \mathrm{M}_{\mathrm{j}}^{\mathrm{l}}} \mathrm{X}_{\mathrm{j}} \tag{4.35}$$

4.6 Proposed Initialization Algorithm

The K-means clustering requires the user to determine the number of clusters and initial centroids. Both these pieces of information are challenging and the details on the number of clusters are beyond this study. Figure 4.8 presents a typical PMU output data (phase a) which has been yielded from a power system scenario. This scenario has been explained in the next section, along with the test case which used for PMU data extraction.

K-means algorithm summary:

- Input: $\boldsymbol{X}$and k as input data set and number of clusters
- Random initial centroids: M_j
- $l = 1$ (first iteration)
  - Calculate objects distances with centroids:$\|X_i - M_j\|^2$
  - Compare the distances and update the clusters:$\boldsymbol{M}_j$
  - Terminate if no change in clusters' members.
  - Update the centroids: M_j^{l+1}
  - $l = l + 1$, go to 4th line

Figure 4.7 K-means Basic Algorithm

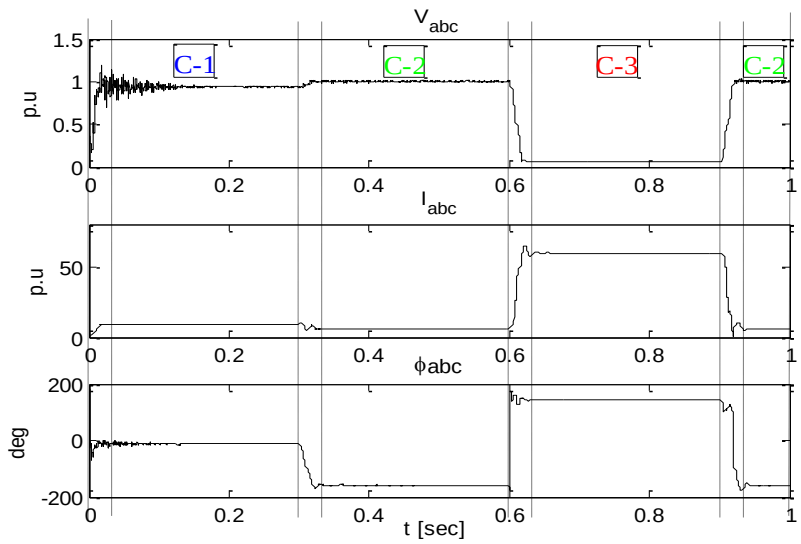

Figure 4.8 PMU 5 Data for a Scenario

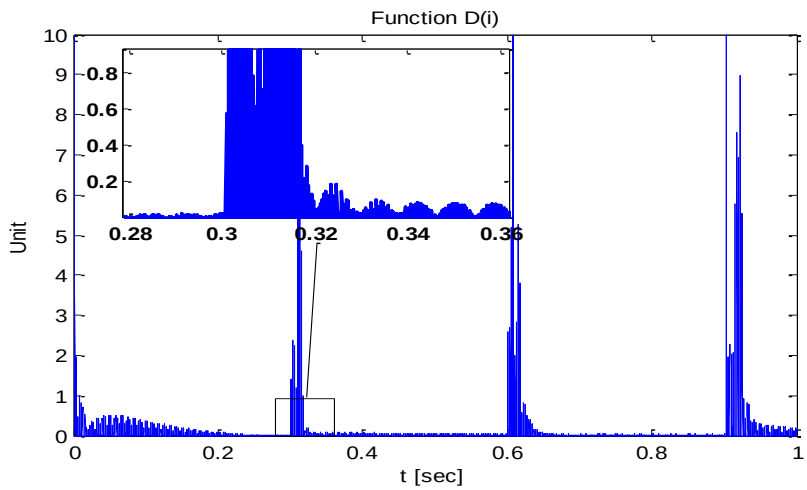

Figure 4.9 Discrete Function D(i) Representing the System Step Length

As mentioned before, each category of data has its particular traits due to its natural system and field. Dashed lines in Figure 4.8 separate the different phases of working in our system as the scenario events are happening in 0 to 1 second simulation time spans. Plotted curves fall into 4 categories, three of which are C-1, C-2 and C-3 and are related to the system when it is stable. Narrow bands in Figure 4.8 followed by dashed lines represent the transient time in which the system encounters a change or fault and needs to pass a time to be dampened. Figure 4.8 comes from a stream set of data with 24,031 points yielded by a PMU. It should be mentioned that as opposed to medical or other fields, order of data exists in PMU output and matters in this study. This is how each X_i ($1 \leq i \leq 24031$) relates to a specific moment and is a dot with its position in a system trace. Figure 4.10 presents the same data in a 3-D plotted environment using dots to curve the data. Cyan colored dots in Figure 4.9 are related to narrowly dashed

line times in Figure 4.8 and in the same manner exist for C's and their colors. One can deduce that Figure 4.8 narrow bands in trivial times result in far spaces in actual 3-D space. That is, transient parts take a small amount of time but the plotted system using dots results in a bigger step length for dots for those time periods. This phenomenon is true for faults, change in load, DGs disconnection/connection, and any other disturbance or work condition alteration in power systems. PMUs samples the phasors in a constant sampling rate, synchronized by satellite GPS. Hence, any change in Figure 4.10's dots' step length is merely due to the system's response, which can be categorized based on the change and average step change. For instance, in Figure 4.10 the upstream utility grid feeds the system in C-1. Connecting a significant amount of DGs to the system changes the system working point, moving it from C-1 to C-2. After stabilizing in C-2, the system encounters a fault and enters into C-3. Moving the system's working condition in Figure 3 from C-1 to C-2 is by close dots with small steps, however dots are running from C-2 to C-3 which indicates a fault. Also power system and PMU output data have a concentration of data points in a steady state condition. That is why we have more than 5,000 data points in each of C's sections while all the cyan parts number less than 1,500.

These two PMU data traits, data step length, and concentration have been considered to find the best initial centroids with the simplest procedure. A discrete function has been used to calculate every step length of the system. Function D(i) is

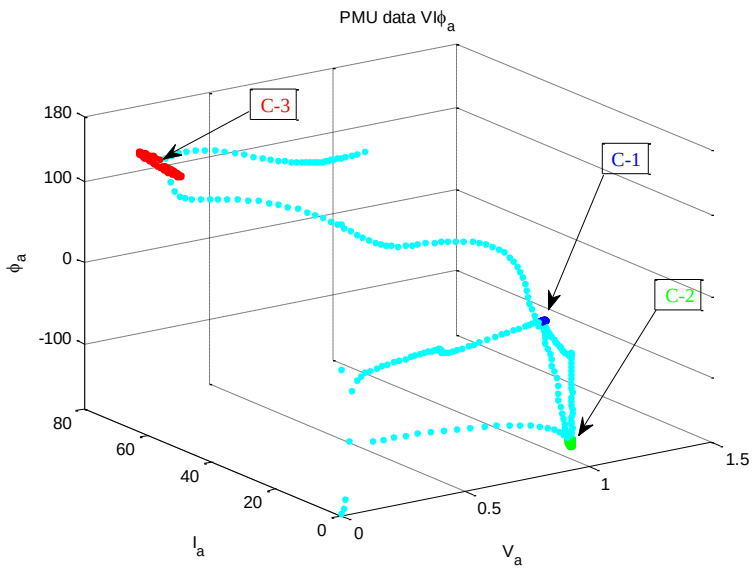

Figure 4.10 PMU 5 VIϕa 3-D Data Presentation

shown here:

$$\mathrm{D(i)} = \|\mathrm{X_i} - \mathrm{X_{i-1}}\| \tag{8}$$

When $1 < i \leq n$ and subsequently the length of D(i) is always one less than length of data set. Figure 4.9 illustrates the resulted function for Figure 4.9's PMU data and undergone scenario. As you can see, the value of D(i) for the i's which are located in the transient time periods are significantly more and sometimes abnormal compared to other times. Figure 4.9 and the magnified section clearly presents that during the steady state operation the data points' step length barely exceed 0.2 with an average in the range of 0.05. But when the system changes its phase of working operation point, this step change significantly increases to more than 1.

Using the function D and the PMUs data traits enabled us to develop the innovative and practical proposed algorithm for calculating the best initial centroids location.

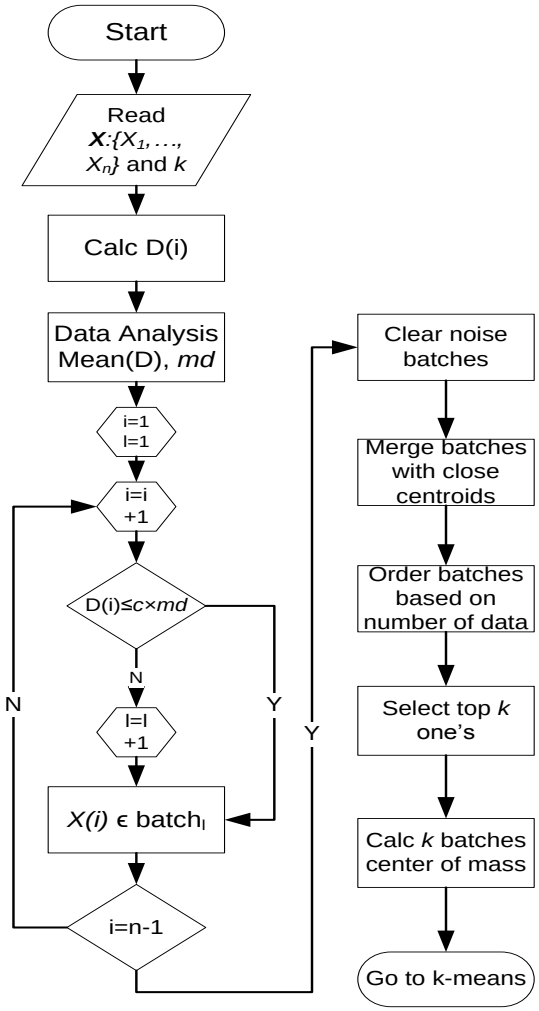

Figure 4.11 Proposed Initial Centroids Calculation Algorithm Flowchart

Figure 4.11 shows the flowchart for the algorithm which has been proposed and utilized in MATLAB programming environment to determine the best initial centroids. After reading the user provided set of data X and the demanded number of clusters (k), function, D(i) is being calculated in the third executing stage. In the fourth section the mean value of the D function will be calculated and called md. md plays a significant rule in the algorithm result, efficiency, and adjustment. It can be seen that the single and main loop in the algorithm judges the data based on this value. As a matter of fact this algorithm can be used in other fields having the same traits which have been mentioned in previous paragraph by regulating the value of md and c to increase the accuracy and to avoid the loss of important data. Another task in this stage is the data analysis which evaluates the data dimension, scales, and important parameters such as data density and diversity in the space of R^d. All values of the D function will be evaluated in the algorithm loop section. Taking advantage of MATLAB programming by string coding enables us to have an undefined number of batches. Figure 4.10 and the dot's step length has been used in the algorithm loop. That is in this loop each group of X's which have a D value less than $c \times md$, i.e. the points have a common and relatively small step length, fall into a batch. However for being conservative about this, the c coefficient will be chosen tightly to have a bigger number of batches but not to mixing X's which may not belong to a same cluster. Increasing the i in the loop if the current D(i) didn't meet the condition, a new batch will be created and next points will fall into this batch unless the loop meets the termination condition or a point step length (D) won't meet the core condition again, resulting in another batch. As mentioned in the last paragraph, c and md are the parameters which led us to regulate and adjust the algorithm either for PMUs and power system applications or for any other fields for which their data have the same traits as discussed. In this application the total number of data points is 24,031, therefore batches with sizes less than 100 can be easily considered as noise or at most unnecessary. It should be mentioned that we have reached the same results by ignoring batches sizes of 1,000 but 100 will be the most conservative batch reduction size. The algorithm merges the batches with close average points. This is not really critical in real systems, as we assume we will have enough data during normal working conditions and abnormal working conditions have smaller periods of time compared to the normal, steady state. Pushing the algorithm to the edges of this section has been done using the data scale analysis section which

gives the algorithm an idea about how far the clusters may exist, taking the data density into account. After this stage, we have a limited number of batches each of which includes sets of data with certain distance of their average. These batches will be organized in a rising manner based on their sizes. Obviously, batches with larger sizes have more importance for us at least as far as indicating clusters with bigger sizes. Finally, the top k ones of these batches will be chosen to represent the clusters and their center of mass will be calculated. These centroids will be used for K-means initial centroids significantly improves it as it will be explained and shown in next section.

4.7 PMU Data Clustering

A simplified 8-bus system has been used in this study for simulations and PMUs' raw data extraction. SDFT PMU has been used in to estimates the voltage, current, and phases of the installed bus with specific sampling frequency. The 8-bus system is a

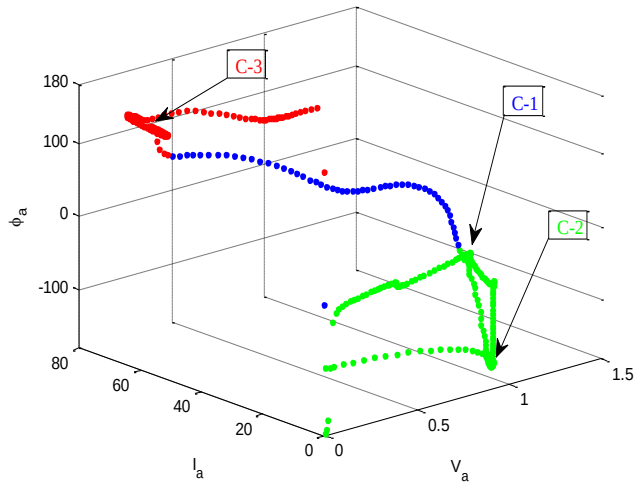

Figure 4.12 PMU 5 Clustered by Basic K-means

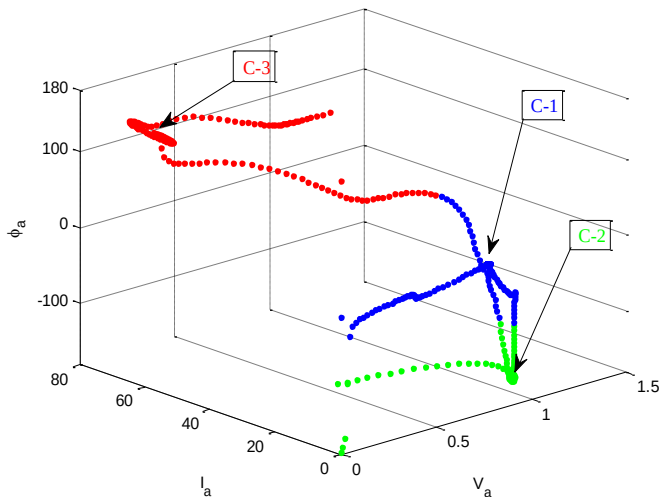

Figure 4.13 PMU 5 Clustered Using Proposed Algorithm

radial which is fed from the upstream utility grid (UG) connection. In downstream feeder, it has a large amount of DG which connects at the scenario's second period. The designed scenario aims to show how the system's working state changes and how the PMU data and subsequently proposed algorithm responses change. Figure 4.8 can clearly present the scenario starting from t=0 with normal condition and just being fed from UG. At t=0.3, the downstream DGs connects to the network improving the voltage, reducing the sensed current, and significantly changing the phase in that specific bus. At t=0.6, a bolted 3-phase happened in the middle of the network which is noticeable through the PMU output and will be cleared at t=0.9. After fault clearance, the system is still being fed from both sides. This is the system that has the same state as the second period marked by C-2 sign in green.

Figure 4.9 illustrates PMU 5 VIϕa data plotted based on the known scenario periods. Hence the transient parts are in cyan and the actual clusters have been categorized by different colors and arrows showing the cluster names which are the same in other PMU 5 cluster results. The cyan colored data is to clarify the borders and system states (on bus 5) presented in 3-D $R^d$for the designed scenario. Figure 4.12 presents the clustered data using the basic K-means algorithm and Figure 4.13 shows the resulting clusters using the proposed algorithm. One can observe in Figure 6 that the basic algorithm could not differentiate the C-1 cluster region and specified parts of the transients to it. However the actual C-1 has been included in the green cluster section as of C-2 which is not correct. On the other hand, Figure 4.13 clusters using the proposed algorithm have distinct borders and correct cluster regions compared to Figure 4.9. Using the basic algorithm took 8 iterations while taking advantage of the proposed initialization algorithm reduced it to 9 iterations. Decreasing the iterations by one third has a significant impact on the clustering computational burden on applications.

It is worth mentioning that in power system applications, Central Protection Unit (CPU) may utilize different data combinations. Figure 4.8 illustrates 3 plots of data (VIϕ) that can each be expanded to phases abc. The same thing is applicable using the signals' sequences. Now any combination of this data can be used for decision making and clustering processes regardless of the number of dimensions. The proposed code has no limitation in data dimensions which enables the CPU to utilize any combination of preferred data.

Figure 4.14 and 4.15 present clustering results for the same scenario but use data from PMU3. Figure 4.15 depicts the clustering result from using the proposed algorithm for 3 scenario periods. Connecting the DG at t=0.3 resulted in the system state going from C-1 to C-2 and has a minor location change based on bus 3 signals. Hence, the installed PMU at bus 3 has been chosen, as C-1 and C-2 are located close to each other which is more challenging for clustering. Clustered data in Figure 4.15 shows the correct distinction between C-1 and C-2 knots. However Figure 8 illustrates how K-means may result in a totally incorrect result as of random initial centroids. That is, both C-1 and C-2 knots have been classified inside a single cluster, the parts of which transient have been mistakenly considered as the third cluster. Using the basic K-means method yields results by 9 iterations while the proposed algorithm again decreases it by one third. Data pre-analyzing by proposed algorithm results in precise

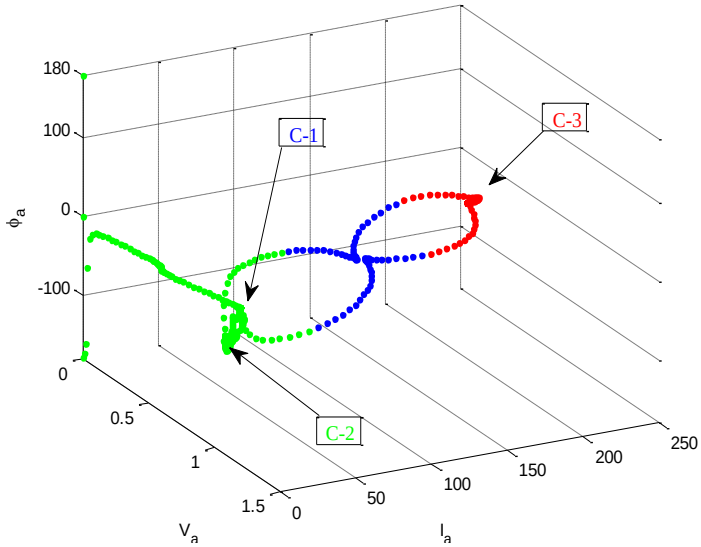

Figure 4.14 PMU 3 Clustered by Basic K-means

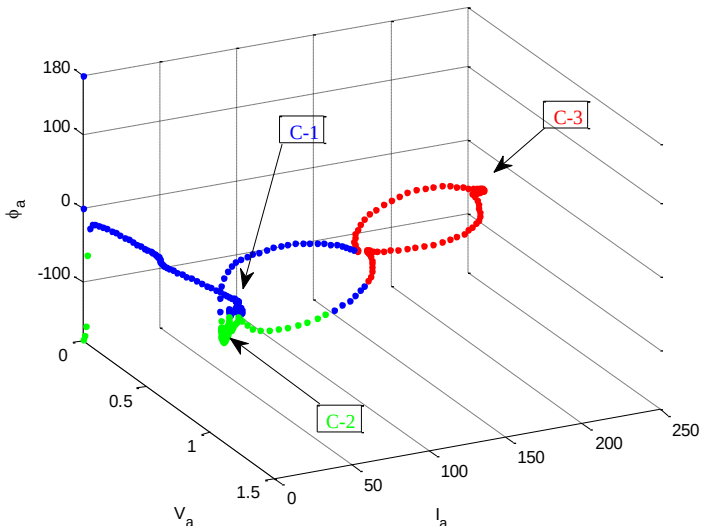

Figure 4.15 PMU 3 Clustered Using Proposed Algorithm

and stable clustering in any number of executions. It has been mentioned before that K-means clustering uses the basic algorithm and does not have a stable output. That is, Figures 4.12 and 4.14 are two selections from many executions which have been made by the author. The basic code may even result in really accurate clustering output or aims to a totally surprising clustered data as of local minimums in objective functions. However the number of iterations never reaches less than two times the number of iterations using the proposed algorithm. Figure 4.16 presents a complicated scenario case which has been clustered using the proposed algorithm. In this complicated fault scenario we have four faults happening which have been added to the steady state working situation result in 5 clusters. These clusters have been represented as C1 to C5 in the plot. Faults happen with 0.2 second intervals (the system is in a steady state condition C3 in this states) and each of them stays in the system for 0.2 second as well. This cluster result has been yielded by 6 iterations when same clusters' region and iterations have been yielded in any execution. On the other hand, the basic algorithm has significantly different cluster regions per each execution with some critical mistakes in categorizing two cluster knots in a single cluster in many runs. Basic code takes a number of iterations with a minimum of 21 and a maximum of 48 observed and the iteration average total of 34 runs, which is really high compared to 6 iterations using the proposed algorithm.

4.8 Conclusion

In this section a new algorithm has been developed to pre-analyze the data and

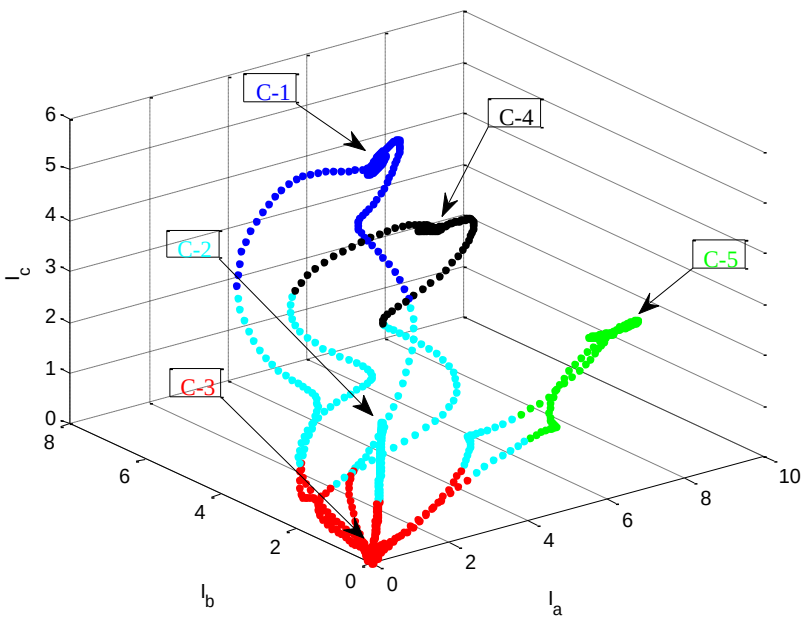

Figure 4.16 Clustered Using Proposed Algorithm

calculate the initial centroids for clustering using K-means. K-means clustering has a significant importance in our proposed CPU as well as in many other applications. Each application's data has its special traits. Basic K-means clustering simply uses randomly chosen data to start with as initial centroids. This results in unstable and inaccurate in clusters in big iteration numbers. The proposed algorithm takes advantage of the power system PMU data characteristics to evaluate the scales of the data and calculate the most efficient initial centroids. This approach significantly reduces the number of iterations and stabilizes the clustering output. That is, the clustering regions no longer vary in each execution. The effectiveness of this algorithm can be used in CPU for power system online protection applications. The algorithm is simple and does not add a significant computational burden to the system and can be considered for fast and transient applications.

Chapter Five

Central Protection Unit (CPU) for Smart Grids with Decisive Private DGs

5.1 Overview

Current power systems are taking advantage of systems such as WAM and SCADA (supervisory control and data acquisition) for supervising networks in case of disturbances or oscillations. These supervisory systems are barely effective as they are unable to manipulate the system equipment and take action instantly. Actually SCADA can be described as a data acquisition, monitoring, and archiving center which technically facilitates one of the vital inputs for innovative CPU.

On the other hand, the current power systems are heading towards integrating DGs as much as possible with private owners who are deciding about the generation time schedule. This means system structures and generation points are constantly changing and networks should be able to be flexible to the changes by adapting with the new structures. With any significant changes in downstream feeders or generation plants the amount of power transfer and direction alter. Subsequently, protective elements and relay characteristics need to be corrected. This task should be done by sending crews to various sites and substations nowadays. One of the CPU's tasks is to remotely manipulate relays' characteristic coefficients. Inventing digital relays such as Simens SIPROTEC family, SEL Relays, and GE's D series relays manipulation is more affordable, there are still many other limitations. The more important issue is to reach the point of diagnosing the network state as discussed in previous chapters.

With the integration of SERs into the power networks, islanding would be one of the choices to take advantage of DGs benefits. By islanding some regions within faults instead of disconnecting a large area, we would isolate the faulty line and the islanded region can keep on feeding loads while standing alone. In the invented CPU central logic, some definitions such as load priorities have been considered which have been explained. These all are feasible by taking advantage of various sections discussed in previous chapters which are DG impacts on Power Systems, Digital Relays, PMU algorithms, PMU data analyzing, K-means clustering and other mathematical approaches for mining PMU data such as higher order indices such as kurtosis and skewness. These are all parts of the CPU's central decision making system, but they also need more sections to cooperate with each other and provide supportive information. This chapter describes the proposed algorithm and structure called CPU

and how it can be adapted to the current systems in order to build a smart protection unit for smart grids.

5.2 CPU Description

The picture bellow illustrates the general overview of CPU and its complementary systems. Details and technical complexities have been avoided in this figure to depict a prospective overview of the proposed CPU. Various systems are connected to each other through the CPU to provide it with needed information. Some of these systems, which have been covered in this study, are already being used and the CPU employ them with minor adjustments. This is one of the benefits of the proposed CPU, that it uses almost all the capacity and equipment already installed in power systems.

5.2.1 Off Line Data

Recent advances in science and technology have been fast, effective, and innovative which should be considered in any new design. Off line data sections in the CPU prototype play an important role regarding critical information needed for any decision making. This information consists of three parts:

- Load Prediction and Power Flow
- Generation Units Data
- Power Systems Specification

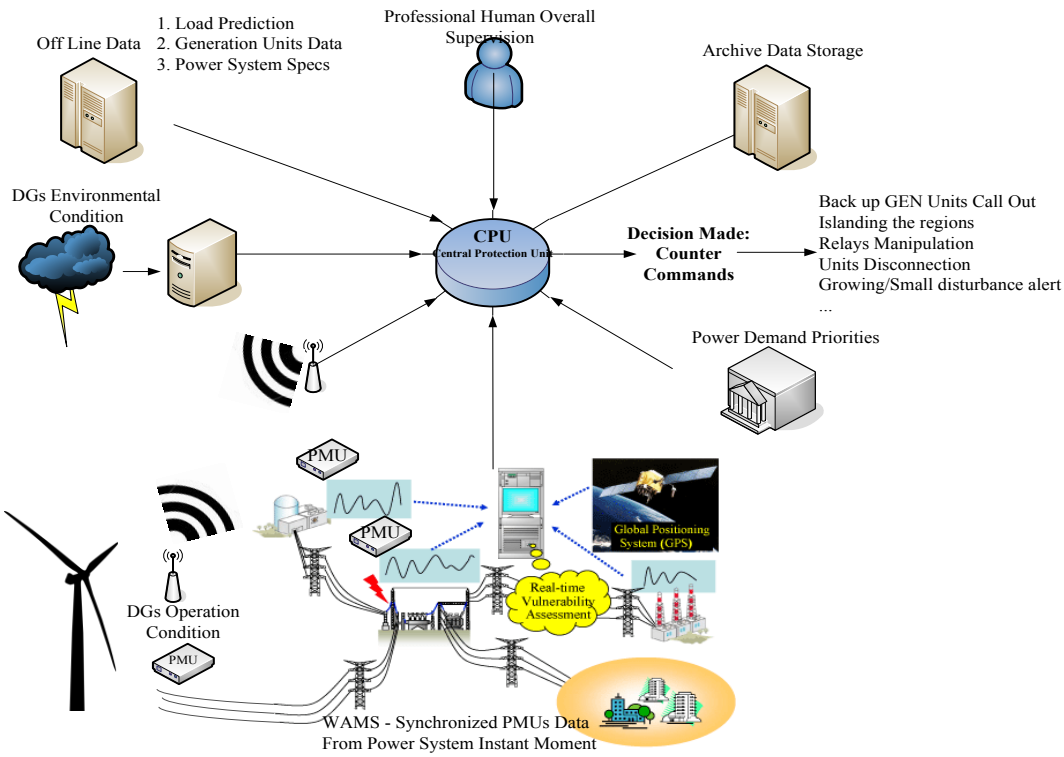

Figure 5.1 Central Protection Unit (CPU) Overview

Load prediction is absolutely vital for power flow calculation and the CPU. However, it can be calculated in a timely manner outside of the CPU task in order to reduce the processing time needed to reach a decision. It should be mentioned that facilities doing this process are currently available and operational in power systems. These just need to be adjusted with CPU and to be equipped by communicational means to send their output for CPU off line data storage centers.

5.2.2 DGs Environmental Condition

Natural disasters are one the causes for outages, especially for systems working on the boundaries resulting in blackouts. Scanning the earth via satellite for either forecasting or tracking the weather and environmental conditions is quite conventional at present. Having this data in the input, CPU has already run various scenarios which might happen. Therefore in cases of faults or disturbances the response can be broadcasted in less than a cycle all over the system and be imposed in less than 3 cycles. The fault/disturbances can be either a disconnection of the DGs that are working in the severe weather condition or started by any ordinary faults in other places tending to deteriorate with some vulnerable units in the system. Another use for this information is that CPU can call out for standby DGs to be replaced by environmentally affected units in case of optional or obligatory disconnection to avoid power disruptions for even the slightest moments.

5.2.3 Authority Load Priority

This section is about the information provided by the government based on the country's current situation. A country, region, or continent based on the environmental, economic, political or geographical situation can be critically more dependent on some particular load. Also a country might even be in favor of some special region or area electrical load because of being in the middle

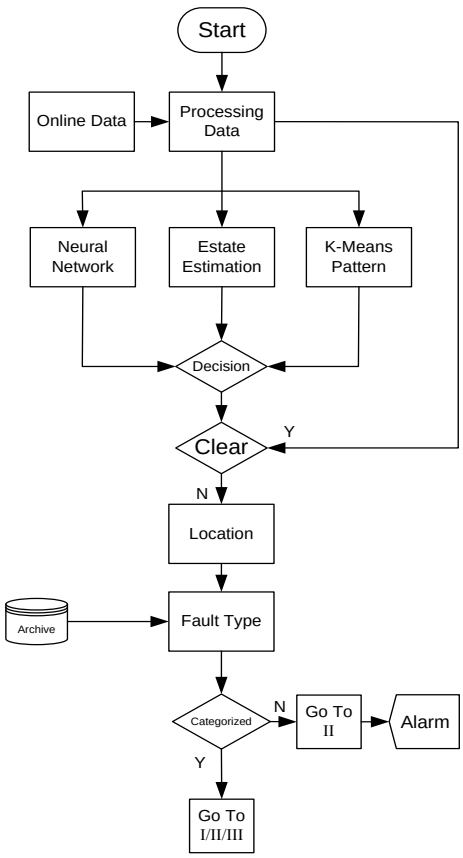

Figure 5.2 Central Diagram

of an ongoing strategic situation. This means the priority of that region’s loads is too high that the rest of the region's power reliability can be sacrificed. The amount of value and priority which is given to such an area and region can be defined by the governmental authority and attributed using weight indices. This can be considered in best islanding calculations and graph generation. This information consists of load priorities which should be considered in islanding calculation. This can be a critical industrial plant that’s disconnection will affect the country’s economy or even a military bases, which are required to be uninterruptedly fed. In this case, the CPU will not disconnect the high demanded load or at least considered it as a well fed, stand-alone island.

5.2.4 Online Data

In the CPU prototype, Online Data refers to all the systems and infrastructure gathering raw information from power systems in current operation. These systems are SCADA, WAMS, DGs Coupling Point, and PMUs all over the network. SCADA gathers information from all network substations using Ethernet. The most important role of SCADA is being connected to all digital relays, SF6 circuit breakers, and RTU equipment to make it eligible as a perfect command career. This means in case of any change in DGs topology or islanding, it is SCADA which take the responsibility of imposing the changes by transmitting the command to devices. DGs coupling point online data stream plays as a check signal for CPU. CPU is significantly focused on being flexible to change in DGs topology, whether obligatory or not, i.e. as an optional decision by DG owners. This is why one of the important advantages of this system is being adaptive in case of decisive DG owners.

Figure 5.2 depicts the flowchart which CPUs decision making uses along with information needed for its task. One can pay attention to where online data has been placed, which illustrates their importance in CPU processing center as well as three separate decision making methods. These accurate methods are:

- Neural Networks
- State Estimation
- K-means Pattern Recognition

PMU constant stream of data plays a major part of these decision making methods. Its accuracy during steady state and fault condition and its ability to track the aimed

values during severe fault is highly improved by this invention. This is why a tremendous amount of time and care has been spent on discussing, designing and improving PMUs. This has resulted in the state of the art DFT and SDFT PMUs that have the ability to track the frequency and estimate the phase with fewer than 10^{-4} errors during the faults and disturbances in an ideal design. This accuracy and ability in tracking the signals precisely enables us to implement mathematical methods such as State Estimation and K-means Clustering. For instance Figure 3 depicts PMU data processed and categorized by K-means clustering. Method strength is clear in categorizing PMU's data for a scenario consisting of 4 faults in row.

Figure 5.2 depicts the flowchart of the CPU main processing algorithm. One may notice that decisions made in CPU have been based on a parallel system investigation using three separate methods. In unanimous situations the decision security is not an issue. However there will be cases in which various combinations of decisions may result in separate methods. Based on various working conditions and accuracy limits, violation in Online Data stream a weighting index will be attributed to each of the results. Therefore, the final system state will come out as a matter of working condition and method robustness in various cases along with indices attributed to it.

The main CPU processing and logic core determines the state of the system and whether or not there is an abnormal sign. Online data

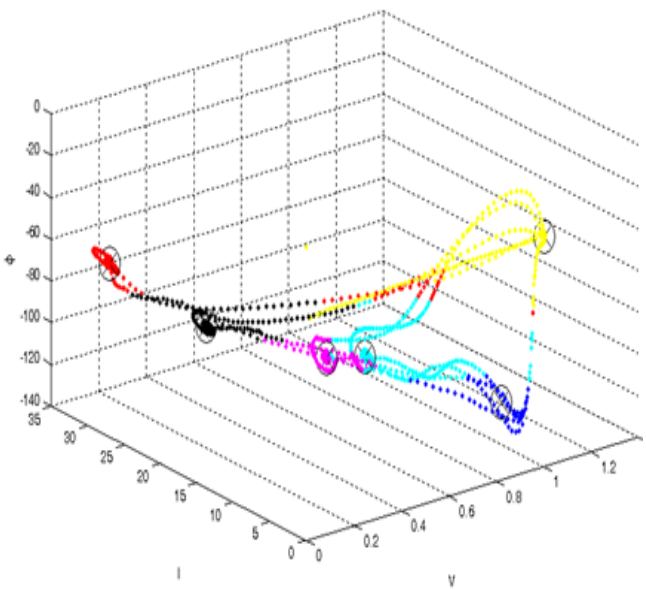

Figure 5.3 K-means Clustering for a Fault Scenario

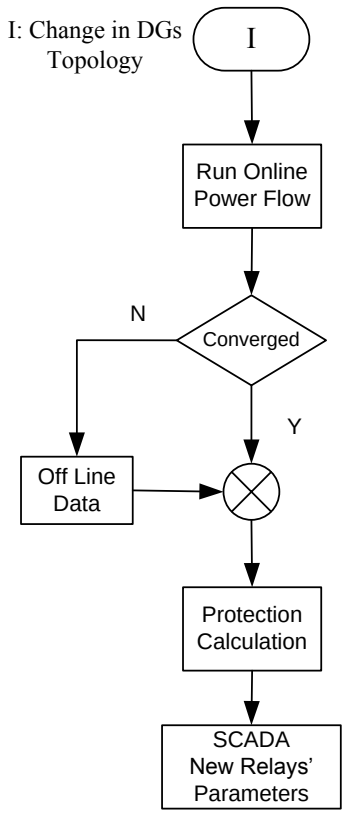

Figure 5.4 I Change in DGs Topology

continuously feeds into the CPU's central processing logic to provide it with raw. When using three parallel disturbance diagnosis systems a fault or disturbance will be easily noticed. In the next stage, CPU will locate the fault point or region using PMUs data. It should be mentioned that different fault and disturbances would have various effective areas, speeds of impact and approaches to locate. For instance a single line to ground fault can be detected using PMUs abrupt change in phase, current, and voltage which engages a couple of buses and the faulty transmission line. While small, the signal instability initiated from a single bus or machine can involve a wide region. An interesting point in here is that using off line data and online load and generation acknowledgments, CPU can easily decide whether a system change resulted from a fault or not. This is because CPU already has an expectation of operating system based on online and off line data.

Fault type will be detected by designing robust algorithms that are already watching the system state path. Also archived data has been used both to constantly train neural networks and also for updating pattern recognition algorithms. For instance, in Figure 5.5 a preferred state estimation plot lead to using PMU data using Vφf signals. A 4

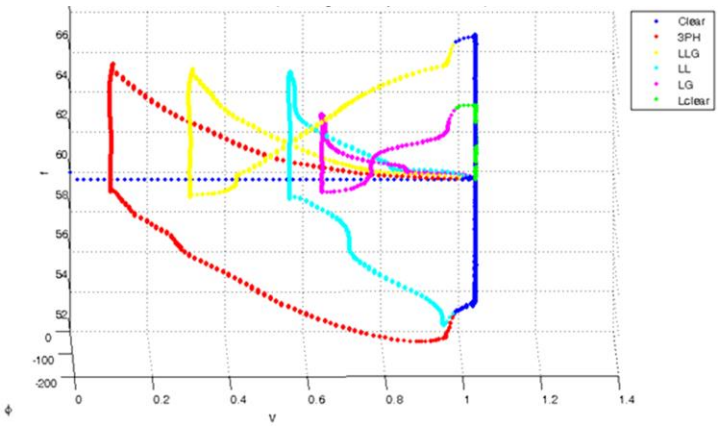

Figure 5.5 System State Estimation Using Vφf Signals

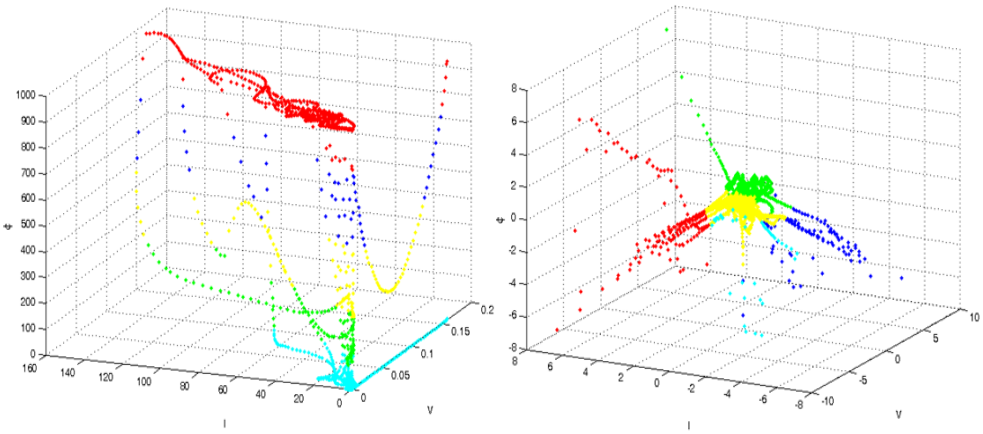

Figure 5.6 a) Kurtosis and b) Skewness Indexes

faults scenario with clear time durations has happened on the system where it is clear that the CPU easily diagnosed all the faults and phases. Taking advantage of Kurtosis and Skewness indices in order to analyze huge amount of data coming from PMUs and WAMS systems is another mathematical option. Therefore, these two statistical data analyzers have been employed as one of the parallel and independent fault and disturbances detectors. These indices have been shown in Figure 5.6 for the same fault scenario as Figure 5.5.

5.3 Conclusion

This thesis has covered power system's various structures and their special characteristics in the initial sections. Various DG types and their characteristics during the normal condition and their responses in case of fault scenarios have been presented based on references and previous studies.

It has been shown in chapter 3 how DGs integration alters the system voltage, normal and faulty current, power transfer in lines, and stability. It has shown that SDFT algorithm based PMU is the most suitable synchronized measurement device for CPU protective goals. K-means clustering showed the best performance and adaptivity in categorizing the PMU output data. K-means issue regards the number of clusters and random initial centroids have been solved by the data pre-analyzing SIC algorithm. Skewness and Kurtosis have been discussed and used as higher order indices for disturbance fast diagnosis. These indices have a higher speed and lower reliability. That is why the reliability weighting index has been introduced in last chapter to judge parallel diagnosis approaches with different outputs. Chapter 5 narrowly introduced the proposed CPU that facilitates smart protection for smart grids.

5.4 Future work

This research work investigates a major challenge in power systems. Some aspects of this research work are complimentary sections to the proposed CPU which can be chosen as future research topics in this field.

- Investigating power market and CPU possible impacts
- Communications rate and its obstacles in CPU especially for transient stability
- Using graph theorems for evaluating the best DGs connecting matrix and islanding
- Using high dimensional data in K-means clustering algorithms
- Storage devices such PHEV and their impacts on the CPU

References

[1] Barker, De Mello, "Determining the impact of distributed generation on power systems. I. Radial distribution systems," *Power Engineering Society Summer Meeting, 2000. IEEE*, vol.3, no. pp.1645-1656 vol.3, 2000.

[2] B. Matic-Cuka, M. Kezunovic, "Improving Smart Grid Operation with New Hierarchically Coordinated Protection Approach" *The 8th Mediterranean Conference on Power Generation, Transmission, Distribution and Energy Conversion (MEDPOWER 2012)*, Cagliari, Italy, October 2012.

[3] Cheng, Shirmohammadi, "A three-phase power flow method for real-time distribution system analysis," *Power Systems, IEEE Transactions on*, vol.10, no.2 pp.671-679, May 1995.

[4] Butler-Purry, Marotti, "Impact of Distributed Generators on Protective Devices in Radial Distribution Systems" *Transmission and Distribution Conference and Exhibition, 2005/2006 IEEE PES*, vol. no. pp.87-88, 21-24 May 2006.

[5] Dugan, Kersting, "Induction machine test case for the 34-bus test feeder description" *Power Engineering Society General Meeting, 2006. IEEE*, vol. no. pp.4 pp.

[6] Distribution Test Feedrs Working Group, IEEE PES Distribution System Subcomittee [online]. Available: http://www.ewh.ieee.org/soc/pes/dsacom/testfeeders/index.html.

[7] U.S. Department of Energy (DOE), http://energy.gov/articles/national-energy-action-month

[8] "IEEE Recommended Practice for Protection and Coordination of Industrial and Commercial Power Systems" IEEE Std 242-2001 (Revision of IEEE Std 242-1986) [IEEE Buff Book], vol. no. pp.740, 2001.

[9] Schweitzer Engineering Laboratory (SEL): https://www.selinc.com/SEL-551/.

[10] Dugan, McDermott, "Distributed generation" Industry Applications Magazine, IEEE, vol.8, no.2 pp.19-25 Mar/Apr 2002.

[11] Chiradeja, Ramakumar, "An approach to quantify the technical benefits of distributed generation" Energy Conversion, IEEE Transactions on, vol.19, no.4, pp. 764-773, Dec. 2004.

[12] Baran, El-Markaby, "Fault analysis on distribution feeders with distributed generators" *Power Systems, IEEE Transactions on*, vol.20, no.4 pp. 1757-1764, Nov. 2005.

[13] Massoud, Ahmed, Finney, Williams, "Inverter-based versus synchronous-based distributed generation; fault current limitation and protection issues" *Energy Conversion Congress and Exposition (ECCE), 2010 IEEE*, vol. no. pp.58-63, 12-16 Sept. 2010.

[14] Nimpitiwan, "Inverter-based photovoltaic distributed generations: Modeling and dynamic simulations" *TENCON 2010 - 2010 IEEE Region 10 Conference*, vol. no. pp.7-12, 21-24 Nov. 2010.

[15] Keyhani, Toliyat, "Flying-capacitor boost converter" *Applied Power Electronics Conference and Exposition (APEC), 2012 Twenty-Seventh Annual IEEE*, vol. no. pp.2311-2318, 5-9 Feb. 2012.

[16] Abu-Hashim, Burch, Chang, Grady, Gunther, Halpin, Harziadonin, Liu, Marz, Ortmeyer, Rajagopalan, Ranade, Ribeiro, Sim, Xu, "Test systems for harmonics modeling and simulation" *Power Delivery, IEEE Transactions on*, vol.14 no.2 pp.579-587, Apr 1999.

[17] IEEE Standard 399- 1990, "IEEE Recommended Practice for Industrial and Commercial Power System Analysis" IEEE, New York, 1990.

[18] Willis, "Analytical methods and rules of thumb for modeling DG-distribution interaction" *Power Engineering Society Summer Meeting, 2000. IEEE*, vol.3, no. pp.1643-1644 vol. 3, 2000.

[19] Qiuye, Zhongxu, Huaguang, "Impact of Distributed Generation on Voltage Profile in Distribution System" *Computational Sciences and Optimization, 2009. CSO 2009. International Joint Conference on*, vol.1, no. pp.249-252, 24-26 April 2009.

[20] Jun-Zhe, Chih-Wen Liu, "A precise calculation of power system frequency and phasor" *Power Delivery, IEEE Transactions on*, vol.15, no.2 pp.494,499, Apr 2000.

[21] De La Ree, Centeno, Thorp, Phadke, "Synchronized Phasor Measurement Applications in Power Systems" *Smart Grid, IEEE Transactions on*, vol.1 no.1 pp.20-27, June 2010.

[22] Jun-Zhe, Liu, "A smart method makes DFT more precise for power system frequency estimation" *Power Engineering Society 1999 Winter Meeting, IEEE*, vol.2 no. pp.909-913 vol.2 31 Jan-4 Feb 1999.

[23] Darwish, Fikri, "Practical Considerations for Recursive DFT Implementation in Numerical Relays" *Power Delivery, IEEE Transactions on*, vol.22 no.1 pp.42-49 Jan. 2007.

[24] Lobos, Rezmer, "Real-time determination of power system frequency" *Instrumentation and Measurement, IEEE Transactions on*, vol.46, no.4 pp.877-881 Aug 1997.

[25] Karimi-Ghartemani, Boon-Teck, Bakhshai, "Investigation of dft-based phasor measurement algorithm" *Power and Energy Society General Meeting, 2010 IEEE*, vol. no. pp.1-6, 25-29 July 2010.

[26] Morf, Kailath, "Square-root algorithms for least-squares estimation" Automatic Control, IEEE Transactions on, vol.20, no.4 pp.487-497, Aug 1975.

Vita

Pooria Mohammadi was born in Iran in 1987. He studied his bachelor in Electrical Engineering at Iran University of Science and Technology (IUST) concentrating on Power area. He fulfilled his bachelor thesis on FACTS devices which also resulted in a patent after extensive research under professor Shayanfar supervision. He always has been interested in power systems protection, compensation and stabilization. Pooria is currently pursuing his PhD at Louisiana State University (LSU) in power systems and protection laboratory.